DEVELOPMENT OF A STEADY-FLOW JxB ACCELERATOR FOR WIND TUNNEL APPLICATION

By

K. E. Tempelmeyer, A. K. Windmueller,
and L. E. Rittenhouse
Propulsion Wind Tunnel Facility
ARO, Inc.

TECHNICAL DOCUMENTARY REPORT NO. AEDC-TDR-64-261

December 1964

Program Element 62410034/7778, Task 777805

(Prepared under Contract No. AF 40(600)-1000 by ARO, Inc.,
contract operator of AEDC, Arnold Air Force Station, Tenn.)

ARNOLD ENGINEERING DEVELOPMENT CENTE
AIR FORCE SYSTEMS COMMAND
UNITED STATES AIR FORCE

NOTICES

Qualified requesters may obtain copies of this report from DDC, Cameron Station, Alexandria, Va. Orders will be expedited if placed through the librarian or other staff member designated to request and receive documents from DDC.

When Government drawings, specifications or other data are used for any purpose other than in connection with a definitely related Government procurement operation, the United States Government thereby incurs no responsibility nor any obligation whatsoever; and the fact that the Government may have formulated, furnished, or in any way supplied the said drawings, specifications, or other data, is not to be regarded by implication or otherwise as in any manner licensing the holder or any other person or corporation, or conveying any rights or permission to manufacture, use, or sell any patented invention that may in any way be related thereto.

DEVELOPMENT OF A STEADY-FLOW JxB ACCELERATOR FOR WIND TUNNEL APPLICATION

By

K. E. Tempelmeyer, A. K. Windmueller,

and L. E. Rittenhouse

Propulsion Wind Tunnel Facility

ARO, Inc.

a subsidiary of Sverdrup and Parcel, Inc.

Presented at the AGARD Specialists' Meeting on "Arc Heaters and MHD Accelerators for Aerodynamic Purposes", 21-23 September 1964, Rhode-Saint-Genese, Belgium.

December 1964

ARO Project No. PL2287

References to named commercial products in this report are not to be considered in any sense as an endorsement of the product by the United States Air Force or the Government.

FOREWORD

The authors would like to thank the many people who are participating in this development program. In particular, special thanks are due to J. M. Whoric, D. R. Wilson, and J. C. Pigott, who have carried out various phases of these tests; W. P. Harmon, who has designed most of the test apparatus; and W. P. Nichols, who has been responsible for the instrumentation. In addition, the authors are also grateful to W. R. Wimbrow, Dr. J. B. Dicks, and Dr. L. E. Ring, who have influenced this program by many helpful suggestions and stimulating discussions.

ABSTRACT

A description is given of the various aspects of an experimental program which is currently in progress at the Arnold Engineering Development Center to develop a steady-flow, direct-current, JxB accelerator for a wind tunnel driver. Electrical discharge and material tests have been made in a supersonic seeded nitrogen plasma at static temperatures and pressures near 3000°K and 1 atm, respectively. Cooled copper electrodes set flush in a wall could be made to carry sufficient electrical currents to make MHD acceleration feasible and still have negligible erosion. Sprayed beryllium oxide was found to be the best insulation material of those tested for the conditions at which a high-pressure accelerator must operate. The design of a water-cooled accelerator having 117 pairs of segmented electrodes and the initial success of prooftests with a prototype twenty-pair electrode accelerator are described. Electrode current fluctuations and various problems associated with seeding the plasma are pointed out as important problem areas for future work.

PUBLICATION REVIEW

This report has been reviewed and publication is approved.

Donald J. Harney

Donald J. Harney
Major, USAF
Chief, Special Projects Office
DCS/Civil Engineering

Donald D. Carlson

Donald D. Carlson
Lt Col, USAF
Chief, Space Systems Office

CONTENTS

ILLUSTRATIONS

Figure

NOMENCLATURE

A	Electrode surface area
B	Magnetic flux density
E	Electric field
h	Enthalpy
h_o	Stagnation enthalpy at channel inlet
I	Current
J	Current density
L	Electrode spacing
M	Mach number
P	Power
p	Pressure
S	Seeding rate
T	Temperature
V	Voltage or velocity
W_g	Gas mass flow
X	Axial distance
γ	Specific heat ratio
δ	Energy loss coefficient
σ	Electrical conductivity
τ	Mean free time between collisions
ω	Electron cyclotron frequency

SUBSCRIPTS

1, 2...5	Electrode position
avg	Average
ch	Channel
dc	Direct current
ex	Exhaust
i	Initial
s	Sheath
t	Stagnation

1.0 INTRODUCTION

The limitations of conventional gas dynamic test facilities in simulating hypersonic flight have been discussed by Ring in Ref. 1. He also has shown in some detail the advantages and possible extension to present-day testing capability which may be achieved with the use of MHD accelerators. This paper describes (1) the experimental program which is currently in progress to develop a steady-flow, direct-current JxB accelerator at the Arnold Engineering Development Center (AEDC), Air Force Systems Command (AFSC), in the United States and (2) some of the practical problems associated with the operation of such accelerators.

A schematic of the ultimate application envisioned at AEDC for this type of accelerator in a hypersonic low-density test facility is shown in Fig. 1. Air would be initially preheated, seeded, and ionized with a conventional arc heater; then passed through a low Mach number supersonic nozzle into the accelerating channel where much of the energy would be added to the plasma in the form of directed kinetic energy. A post-nozzle would be placed at the accelerator exit to expand the gas to the static conditions which occur in the atmosphere and, in addition, to increase the Mach number. It is ultimately hoped that a MHD-powered facility of this type could provide accurate flight simulation in the altitude-velocity region shown in Fig. 2.

The present research and development program, however, has a far more modest goal; development of an accelerating channel which operates at near atmospheric pressure, produces a velocity ratio of about 2 in a nitrogen plasma stream, and is sized such that viscous effects and end effects are not dominant. Because previous investigators have shown that plasmas may be accelerated by MHD means (Refs. 2, 3, and 4, for example) and because of the success of MHD power generators (Ref. 5), the emphasis in the present program has been directed toward the solution of problems associated with long-duration operation at conditions suitable for wind tunnel application and improvement of accelerator performance, rather than just demonstrating again that acceleration occurs. After several months of work, however, plasma flows have also been accelerated by MHD means at the AEDC.

Manuscript received November 1964.

2.0 OPERATING REGIME

Following an analysis such as that given by Ring in Ref. 1, it was decided that the AEDC accelerator would operate with a near-equilibrium seeded flow. It is believed that, if necessary, it will be easier to make corrections to test data for a small amount of seed contamination than it would for the effect of a highly dissociated, non-equilibrium test medium. Moreover, the use of a low-temperature seeded flow lessens the severe heat-transfer problems and results in a more feasible accelerator geometry. With seeding, the accelerator channel would have to operate at static temperatures of about 2500 to 3500°K to achieve the necessary electrical conductivity. Further, the desired test section conditions (Fig. 2) dictate that the accelerator must operate at roughly atmospheric pressure. As a consequence, the operating conditions of the AEDC accelerator are considerably different than those employed by other groups. Most of the other experimental accelerator work in progress is at much lower pressure levels. For example, Wood and Carter at NASA-Langley (Refs. 2 and 6) are operating accelerators at static pressures of 0.1 atm or less, whereas at Norair (Ref. 4) and NASA-Ames (Ref. 7) accelerators operate at pressures below 0.01 atm.

A computer program has been prepared for quasi-one-dimensional channel flow which includes the MHD effects, as well as those of friction and heat transfer (Ref. 8). With this program the flow and electrical characteristics of families of accelerators have been studied. Some typical operational characteristics of a steady-flow accelerator are given in Fig. 3 and demonstrate that magnetic fields of about 20,000 gauss, electric fields of about 90 v/cm, and current densities up to 70 amp/cm^2 will be necessary to double the velocity in a 50-cm channel. Such an accelerator operating at near atmospheric pressure would have $\omega\tau \approx 2$.

It is expected that about 1 percent alkali metal seed by weight will be needed in such a research accelerator to obtain the required electrical conductivity. Various compounds containing potassium such as K_2CO_3 or KOH as well as NaK (a eutectic mixture of sodium and potassium and a liquid at standard conditions) have been considered as possible seeds. Cesium has been excluded as a possibility because it was felt that it would be too expensive for day-to-day operation of a large MHD-driven wind tunnel.

3.0 TEST APPARATUS

A 2-mw plasma-jet facility has been assembled in order to study various problems pursuant to the development of a MHD accelerator. Some of this equipment is shown in Fig. 4, and a complete description of it is given in Ref. 9.

The development test apparatus employs a Thermal Dynamics 2-mw arc heater to supply a N_2 plasma with mass flows up to about 0.2 kg/sec at stagnation pressures and temperatures of 3 to 6 atm and 4000 to 6000°K, respectively. Typical thermodynamic states of the plasma leaving this arc heater are summarized in Fig. 5. A small stilling chamber is placed at the exit of the arc heater into which the low ionization potential seed material may be introduced. Seeded plasma passes through a M = 1.8 supersonic nozzle which has a 2.5- by 2.5-cm exit geometry. Various test channels or accelerators can be connected to the nozzle exit, placed between the magnet pole pieces, if desired, and discharged into an exhaust tank.

A conventional iron-core, C-shaped electromagnet having 7.6- by 38.1-cm pole faces and a 6.0-cm gap is available to generate the B-field. It is capable of producing fields up to 20,500 gauss on its centerline. The arc heater is powered by a central, rectified, d-c power supply. A separate electrical supply system utilizing 1700 automotive batteries is used to power the accelerator. The batteries are arranged such that separate independent circuits can be provided for each electrode pair in the accelerator. Various axial electric field distributions can also be obtained along the channel with this system.

4.0 ELECTRICAL DISCHARGE STUDIES

Since little information was available concerning electrical discharges in supersonic, seeded plasmas at atmospheric pressure and since electrical discharges are extremely sensitive to pressure, the first phase of the experimental program was to determine what type of discharge would actually occur and to document characteristics. A detailed summary of this work is given in Ref. 9.

Following some preliminary tests with single pairs of electrodes, several multi-electrode channels were constructed with five or six pairs of electrodes set flush in the wall and segmented by boron nitride or beryllia insulators. Two typical discharge test channel configurations

are shown in Fig. 6. Usually, the electrode gap was about 2.5 cm, and the electrodes were powered by separate battery circuits, which were electrically floating with respect to each other. Sidewalls were made of water-cooled copper blocks or strips and covered with high-temperature electrical insulating material. For some tests the sidewalls were removed. These channels were connected to the arc-heater nozzle, and the plasma entered the discharge channel at a velocity of about 2000 m/sec. Tests were made at various plasma enthalpy levels, pressure levels, and seeding rates. Both hot tungsten electrodes which emitted thermionically and cold, water-cooled copper electrodes which had surface temperatures below 600°K were investigated. In addition, two types of seed, saturated solutions of K_2CO_3 in water and liquid NaK, were used. In a few of these discharge tests an orthogonal magnetic field was also applied.

4.1 CURRENT-VOLTAGE CHARACTERISTICS

For seed rates from 0.2 to 2.0 percent (K or NaK by weight) small currents, a few hundredths of an ampere, flow across the plasma with applied voltages as low as a few volts. As the applied voltage is increased, the current increases very slowly at first but then quite rapidly. The discharges have a positive slope up to 100 amp; that is, the discharge does not appear to take the form of a pure arc. A typical voltage-current curve for cold copper electrodes over a wide current range is shown in Fig. 7. Since the very low currents (below 1 amp) are of little interest as far as MHD accelerators are concerned, this range has not been investigated in detail. However, a large number of discharge tests have been made in the high-current range.

Typical discharge characteristics for various plasma enthalpy levels with various amounts of NaK seed are given in Fig. 8. The effects of seeding rate* and pressure level on the discharge are shown in Figs. 9 and 10, respectively. All of these current-voltage discharge curves appear to have a zero-current voltage intercept between about 35 and 90 v, depending upon the enthalpy, pressure, and seeding rate. As previously shown in Fig. 7, the current does not actually fall to zero at these voltages. The apparent voltage intercept probably represents the sum of the electrode sheath voltage drops and the voltage drop across the electrode

*Measured seed injection rates are stated in the figures. These are not necessarily the actual or effective seeding rates because some of the seed material condensed on the cool walls and consequently was not ionized. There is some hope that an equilibrium condensate layer is built up, and after some time interval all of the injected seed goes into the plasma.

boundary layers, and it signals the onset of a different current flow mechanism. The pressure level affects both the level and shape of the V-I discharge curve, whereas the plasma enthalpy and seeding rate primarily influence the level.

All of the discharge results shown in Figs. 7 through 10 were obtained with cold copper electrodes. However, similar current-voltage characteristics were obtained with another test channel containing tungsten cathodes which operated at sufficient surface temperatures to emit thermionically.

Discharges were also established across the supersonic plasma in the presence of a mutually orthogonal magnetic field averaging about 1.55 weber/m^2 over the channel length. Orientation of the magnetic and electric fields was such that the Lorentz force acted in the downstream axial direction. Voltage-current characteristics with the magnetic field were similar to those previously shown; only, a larger voltage (by the amount uBd) is required to achieve a given current because of the necessity of overcoming the induced emf. The induced voltage appeared to increase with increasing current. This may, in part, be due to an increase of the plasma velocity resulting from the accelerating effect of the axial Lorentz force.

Photographs of the discharge with the sidewalls removed, but with the exhaust pressure matched to the average static pressure at the electrode surface, always show very bright bluish-white regions attached to the trailing edges and sometimes the leading edges of the individual electrodes. These bright regions somewhat resemble small arcs and exist on both cathodes and anodes. They appear to be swept rearward, extend into the stream only across the boundary layer, and move in a random fashion laterally across the edges of the electrodes. Movies at frame speeds up to about 3000 frame/sec indicate that the discharge is diffuse through the core or plasma free stream. Water-cooled copper electrodes were only slightly eroded after 20 to 30 minutes of operation and provided the same current at a given voltage as heated tungsten. It seems more probable that since the cathode sheath width is on the order of a Debye length (about 10^{-6} cm for the conditions of these tests), electrons enter the plasma from the cold electrodes by virtue of field emission rather than thermionic emission. However, since large voltage gradients exist at the electrode surfaces and photographs give the impression of arcs across the electrode boundary layers, the possibility of thermionic emission induced by arc attachment augmenting the field emission current should not be overlooked. It is not believed that arc discharges exist in the plasma core. Dicks discusses the electron emission phenomena for the conditions of these tests in detail in Ref. 10.

These tests demonstrated that it is possible to achieve current densities of at least 70 amp/cm^2 with cold-copper electrodes, which is in the range indicated by the theoretical computer studies to make MHD acceleration feasible. Most materials have a rather small temperature interval between their melting temperature and the temperature at which thermionic emission is significant. Maintaining the temperature of thermionic emitting electrodes in this narrow range would appear to be a difficult problem for wind tunnel accelerators which must operate over a range of conditions. In this respect, the water-cooled copper electrodes offer a considerably greater operating flexibility than do conventional thermionic emitters.

4.2 PLASMA CONDUCTIVITY

The nonlinear shape of the current-voltage curves indicates a strong influence of the discharge on the electrically conductivity of the plasma. If the electrical conductivity is identically defined by

$$\sigma = \frac{J}{E} \tag{1}$$

and if σ is dependent on E, one cannot take the local slope of the J vs E curve as representing the conductivity. Consequently, the conductivity is defined below in a manner which satisfied Eq. (1):

$$\sigma = \left(\frac{I}{V - V_s}\right)\left(\frac{L}{A}\right) \tag{2}$$

where L is taken to be the mean geometric spacing between the electrodes and A the electrode surface area. This formulation, although somewhat arbitrary, is believed to be realistic inasmuch as the experimental conductivities evaluated by the use of Eq. (2) agree reasonably well at low currents with the classical equilibrium conductivity calculations given in Ref. 11 (see Fig. 11). Typical values of the conductivity of seeded nitrogen indicated by these experiments are shown in Fig. 11 and demonstrate the strong influence of the electric field. With the available plasma diagnostic tools it is not as yet possible to determine if the conductivity increase is due to joule heating of the entire gas by the discharge or selective heating of the electrons.

For illustrative purposes the experimental conductivities have been compared with predictions from Kerrebrock's nonequilibrium elevated electron temperature theory for plasma which he has called the Two Temperature Conduction Law (see Refs. 12 to 14 for details). This theory assumes that the electrons are selectively heated in the electric field and that the ionization level is in equilibrium with this elevated electron temperature. A coefficient δ appears in the theory which describes the energy

loss from the electron gas by elastic collisions with the neutrals. A comparison between the experimental conductivities and those predicted by this theory for $\delta = 100$ is given in Fig. 12. The agreement between experiment and theory with this energy exchange coefficient is reasonable when one considers the uncertainties associated with the experiment; the plasma static temperature or true seeding rate are not accurately known. From the present results, it may only be stated that there was no evidence to indicate that Kerrebrock's Two Temperature Conduction Law is not valid for nitrogen plasma.

The existence of nonequilibrium conductivities in this pressure and temperature range would be a fortunate circumstance because it would allow a reduction of the operating temperature level of MHD accelerators running at atmospheric pressure, and subsequently, alleviate the materials problem. In any case, these experiments indicate that conductivities of a few hundred mho/meter may be achieved at the desired pressure and temperature levels.

4.3 DYNAMIC DISCHARGE CHARACTERISTICS

Discharge data presented in the previous figures were obtained from conventional d-c meters which damped any high-frequency current fluctuations. Electrode currents, however, were also recorded on a magnetic tape system with a 10-kc response and then re-recorded on paper. These dynamic data show the existence of large current fluctuations. Figure 13 presents a trace of the current fluctuations for various electrode pairs operating at two pressure levels with 1 percent NaK seed by weight. These results, which are typical, show a rather significant amplitude for the fluctuation. With NaK seed the peak-to-peak fluctuations at currents about 50 amp were about ±15 percent of the d-c level without a magnetic field. When K_2CO_3 was used, however, the peak-to-peak current fluctuations without a magnetic field were as high as ±30 percent of the d-c current, whereas with a field of 15,500 gauss, they were reduced to about ±20 percent of I_{dc}. Moreover, it was found that these current fluctuations were distributed in roughly a gaussian manner about the d-c level with a favored frequency of 200 to 300 cps. With NaK seed the prominent frequencies were reduced to about 100 cps.

Figure 13 also shows that a strong correlation exists between the current fluctuations of the various electrodes. From this correlation it is possible to detect a time delay of about 4.8×10^{-5} sec between the fluctuations on electrode pair 1 and electrode pair 5. This time delay corresponds to a velocity of about 600 m/sec based on the axial spacing between the electrodes, which is far less than the free-stream velocity

of about 2000 m/sec. This leads to the conjecture that the fluctuations may arise in the boundary layers and be a manifestation of arcs which span the cooler boundary layers as noted in Section 4.1.

Because these current fluctuations would cause uneven acceleration and flow fluctuations in a subsequent wind tunnel test section, it is felt that they must be eliminated or at least minimized. The AEDC accelerator program has been expanded to attempt to pinpoint the source of these disturbances and to determine their effect upon the flow quality at the accelerator exit. Perhaps the diffusing effect of the magnetic field will smooth the currents, when NaK seed is used, to a tolerable level.

5.0 HEAT-TRANSFER AND MATERIALS STUDIES

During the electrical discharge studies, heat-transfer data to the channel walls were obtained and a great deal of practical experience was gained with respect to the utility of high-temperature materials and fabrication techniques needed to contain a continuous supersonic plasma flow at stagnation temperatures of over 5000°K.

Electrode heat transfer was measured by means of a conventional heat balance on the cooling water. Unfortunately, most of the discharge tests were made over periods of 10 to 30 seconds, but a few special heat-transfer runs lasting two minutes or more were made to allow the water to reach thermal equilibrium (Fig. 14). During these tests the plasma stagnation enthalpy was 1750 kcal/kg, the stagnation temperature estimated at 5500°K, and the static pressure was 1 atm. Moderate heat-transfer rates of up to 1.25 kw/cm^2 are observed, which can easily be handled by backside water cooling. When a discharge is initiated, the increase in heat transfer to the anode is about twice that to the cathode because of the electronic impact. Rough measurements of the surface temperature of the water-cooled electrodes indicate that they operate at temperatures less than 600°K. The electrodes show very little erosion after being run intermittently for long periods, but a slight loss of material does occur at the trailing edges. The electrodes shown on the right side of Fig. 15 have an accumulated running time of over two hours and were used in conjunction with boron nitride insulators; those on the left are spray coated with beryllium oxide (BeO) so that the insulation is an integral part of the electrode, and they have been run for 20 minutes. Figure 16 shows the severe erosion experienced by some uncooled tungsten electrodes (designed for thermionic emission) which were run in the same environment but for a much shorter time period. Tests with these electrodes illustrated the consequences of not maintaining the temperature

of thermionic emitters within the narrow range available for satisfactory operation.

The testing program at AEDC has shown that water-cooled copper electrodes appear to be one solution to the electrode problem in MHD accelerators operating at near atmospheric pressure for enthalpy levels at least to 1750 kcal/kg. They can carry currents up to at least 100 amp with negligible erosion and hence have long life expectancy. This type of electrode has given good service in a small 20-electrode research accelerator designed with the heat-transfer rates given in Fig. 14. Their only disadvantage noted to date is that seed tends to condense on the cold surface and if allowed to accumulate could ultimately cause electrical short-circuiting in segmented electrode channels.

Figure 17 illustrates the insulator materials problem, which at present is more severe than that of the electrodes. The electrical resistivities of several insulating materials are seen to decrease quite rapidly with increasing temperature. The benefit gained by keeping the insulation at low temperature is apparent. All of the materials shown in this figure have been tested in various channels. Two were found to have a sufficiently high thermal conductivity to allow heat transfer through the insulation into cooler parts of the channel and adequately high electrical resistivity: beryllia (that is, beryllium oxide) and pyrolytic boron nitride. Either of these materials is adequate for insulators between electrodes or for B-walls, which must also be electrically insulated since they are exposed to the applied field and axial Hall fields on the order of 50 v/cm. Beryllia is hazardous because of its toxicity, and many special precautions must be taken when it is used: however, it seems to be the most desirable material so far as thermal properties, electrical properties, and durability are concerned. Pyrolytic boron nitride is a desirable material with a very high melting temperature, excellent heat resistance, and thermal shock properties. However, a good way to bond this substance to a water-cooled back plate has not as yet been found at AEDC. Hot-pressed boron nitride and alumina were found to erode or spall badly*.

A comparison of sidewalls insulated with strips of pyrolytic boron nitride about 2 mm thick and beryllia about 0.5 mm thick is given in Fig. 18. Both of these walls were tested under the same conditions and

*A new type of pressed boron nitride has recently become available which does not absorb water. It has a considerably longer life than does the ordinary hot-pressed boron nitride.

for about the same length of time. There was no loss of pyrolytic boron nitride; however, the strips separated and cracked because of differential thermal expansion between the insulating strips and the water-cooled back plate. It is felt that the material is good, but a better way to use it must be found. The performance of the BeO sprayed wall, on the other hand, was excellent; it showed no damage or erosion. Consequently, we have pursued the use of sprayed beryllia both for insulating the sidewalls and for insulation between electrodes.

6.0 SEEDING STUDIES

Three seeding systems have been used during these tests. Initially, powdered potassium carbonate (K_2CO_3) was introduced into the stilling chamber at the arc-heater exit by means of a carrier gas. Electrode current data obtained by photographing d-c ammeters at one-second intervals demonstrate the effectiveness of this seeding system. As illustrated in Fig. 19a, large random current fluctuations existed whenever powdered seed was used.* With the powder seeding unit built for these tests the injection rates were always quite erratic, and the seed was poorly distributed in the plasma. As a consequence this seeding technique was temporarily abandoned.

The second system employed saturated solutions of K_2CO_3 or KOH and water. Aqueous solutions are sprayed under high pressure into the stilling chamber through a small wall orifice. In this case the discharges were found to be much steadier than those obtained with powder seed as shown in Fig. 19b. Data shown in several of the previous figures with K_2CO_3 seeding were obtained using the $K_2CO_3 + H_2O$ solutions. This seed has the disadvantage of introducing unwanted waste material into the plasma which not only decreases the plasma enthalpy but unnecessarily contaminates it. Consequently, a third seeding system was also assembled in which a sodium-potassium alloy (NaK) was injected into the arc-heater stilling chamber through a wall orifice. This material is a liquid metal at standard conditions which burns spontaneously upon exposure to air or oxygen and reacts violently if brought in contact with water. Despite its unfavorable handling characteristics, it is a desirable seed because both the Na and K have low ionization potentials, and the compound is inexpensive and liquid. Utilizing NaK seed minimizes the contamination and degradation of the plasma enthalpy. Electrode currents were somewhat smoother

*These very low-frequency current fluctuations caused by erratic seeding rates should not be confused with the fluctuations described in Section 4.3.

when NaK seed was used than they were with aqueous solutions of K_2CO_3 (compare Fig. 19b with 20). High-frequency current fluctuations were also diminished with NaK seed. Higher conductivities were achieved with NaK seed, but its use created additional operating problems. Both of these liquid seed materials have been used successfully, as have aqueous solutions of KOH. However, all of the injected seed does not remain in the plasma and become ionized. As noted before, some of the seed condenses on the cool channel surfaces. Effective seed distribution even with liquids still remains a problem.

Some additional tests have been made to determine what detrimental effects the seed contamination may have on the flow or aerodynamic measurements made in it. This work has just begun and only preliminary results are available at this time. However, the addition of up to 1 percent NaK or 1 percent potassium (about 4 percent of the mass flow for the $K_2CO_3 + H_2O$ solution) does not appear to affect the distribution or level of the impact pressure in the supersonic plasma, nor does it significantly influence the wall static pressure distribution in a one-dimensional channel. Attempts have been made to determine the effects of seeding on stagnation point heat transfer, which is a much more sensitive factor. These results are as yet inconclusive because the seed condenses on the measuring probes and interferes with their proper operation.

Several water-cooled cylinders have been placed in unseeded and seeded plasma flows to determine qualitatively the chemical corrosive and/or abrasive nature of a seeded flow. Several materials were chosen (copper, stainless steel and copper plated with gold, nickel and chromium) because of their different chemical and abrasion resistance properties. The samples were tested first crosswise to an unseeded flow and then in the plasma seeded with about 2 percent K_2CO_3 solution. After runs in the unseeded plasma, several of the samples showed a slight discoloration, but there was no loss of material. A quite different result was observed with the seeded plasma. The plating was removed, and an appreciable loss of material was experienced in the area exposed to the plasma. The material loss based on frontal area of the sample is summarized below:

Material Sample	Material Loss, $gm/min/cm^2$	Abrasion Resistance
Copper	0.0218	Poor
Gold-plated copper	0.0192	Poor to good
Nickel-plated copper	0.0157	Very good
Chrome-plated copper	0.0116	Excellent
Stainless steel	0.0099	Excellent

The gold-plated sample, which is the most chemically inert of the materials tested, had the highest loss of the plated samples. When a comparison is made with respect to abrasion resistance, it is noted that they are in the order predicted by the known abrasion resistance of the materials. This and the fact that the seeded plasma attacked all the materials tested lead to the conclusion that the process of material removal is mainly abrasive rather than due to chemical reaction. A possible cause of the abrasive action of the seed is that when it is introduced into the plasma, there may be insufficient time for all of the liquid or heavy K_2CO_3 particles to vaporize before they strike the sample.

An obvious implication of these results is that in addition to causing considerable difficulty in maintaining and operating probes in the seeded plasma, models in the test section of a MHD-powered wind tunnel may experience similar effects. Elimination of this problem seems imperative. This work is being expanded to determine if NaK seeded streams are as abrasive as those seeded with K_2CO_3.

At the present time, effective seed distribution is one of the biggest mechanical problems. Several other seeding techniques are being studied, and spectrographic measurements are planned in future tests to determine how the seed is distributed through the plasma.

7.0 ACCELERATOR DESIGN

As a consequence of these preliminary tests, an accelerator was designed to double the plasma velocity. The physical dimensions of the channel were chosen keeping in mind that (1) the channel should fit the available magnet and (2) that friction and end effects should not be predominant. Also, the flow properties entering the channel were dictated by the available plasma generator. An ultimate input power level for the accelerator of 1 mw was selected, and the power supply arranged to provide 60 independent circuits, each of which is electrically isolated from the others.

The accelerator channel has an overall length of 77 cm with an entrance geometry of 2.5 by 2.7 cm. The E-walls are diverged about 1 deg to compensate for the boundary-layer growth, whereas the B-walls are parallel. Water-cooling passages are provided for all the components subjected to heating from the plasma so that the channel could be operated for sustained periods of time. A sketch of the channel is given in Fig. 21.

One hundred and seventeen pairs of water-cooled copper electrodes are provided throughout the length of the channel, but only the center sixty are individually powered by the battery system. Floating non-energized electrodes at each end are used to reduce the inlet and discharge eddy current losses and to electrically insulate the channel from the nozzle and exhaust tank, since large Hall voltages (about 1500 v) are expected. The Hall current is minimized by segmenting the electrodes so that the ratio of electrode gap to electrode length is approximately 10. This results in an individual electrode surface area of about 2.5 by 0.4 cm. A very smooth surface is maintained over the entire length of the wall.

Beryllia, sprayed on four sides of the electrodes and a portion of the surface exposed to the plasma, is used for electrical insulation between the electrodes. The anodes and cathodes are supplied by individual water manifolds which were made of suitable insulating material. Cooling water flow rates of approximately 0.4 gpm are supplied to each electrode.

Copper plates with appropriate water passages and sprayed with a 0.5-mm layer of beryllia on all sides are utilized for the B-walls. The B-wall portion of the channel is comprised of 10 of these sections (five per side) and was segmented in this fashion in order to minimize an accumulation of differential thermal expansion between the beryllia and copper. Moreover, use of sectioned B-walls minimizes the possibility of shorting the channel because of the Hall voltage.

A 20-electrode version of this channel has been assembled in order to carry out proof-tests in regard to the design concept, cooling adequacy, and structural integrity of the full channel. Results of some of these tests are contained in the next section. As of the date of preparation of this report, the full accelerator channel is being assembled but has not as yet been tested.

8.0 20-ELECTRODE CHANNEL TESTS

The 20-electrode channel which has been built and tested is in all essentials the first section or the first 20-percent of the larger accelerating channel described in the preceding section. It is shown with one sidewall removed for illustrative purposes in Fig. 22. The electrodes in this channel form smooth walls and are identical to those being installed in the larger accelerator. For most of these tests the beryllia-coated sidewalls described in the previous section were used, but several successful runs have also been made with sidewalls covered by a 2.5-mm-thick layer of the new type of boron nitride.

Figure 4 shows this particular channel mounted on the arc heater before it was moved between the magnet pole faces. Because of its short length this channel only penetrates a short distance into the magnet and as a consequence, it is in a rather strong B-field gradient. For most of the tests made to date the B-field varied from about 8,500 gauss at electrode pair 8 to about 18,500 gauss at electrode pair 20, and had a mean value of 16,000 gauss in the powered section. Only electrode pairs 8 through 20 are electrically powered. Electrode pairs 1 through 7 are left electrically floating, since the magnetic field in this region is weak, and they are used to isolate the powered electrodes from the nozzle.

Tests were carried out in a nitrogen plasma seeded with 0.9 to 1.5 percent K by weight (in the form of K_2CO_3 and water). The plasma had a mass flow rate of about 0.1 kg/sec, an enthalpy level of 1600 kcal/kg, and a static pressure and velocity at the accelerator entrance of 0.60 atm and 2000 m/sec, respectively. The accelerator was first operated as an open-circuited generator in order to determine the induced voltage distribution, which varies from about 25 v at electrode 1 to 120 v at electrode 20 because of the magnetic field gradient. Various constant voltage increments were then added to the induced voltage level and applied to the powered electrodes. The input power to the accelerator was continuously increased in small steps to a total input power of 0.18 mw, and the channel was taken apart frequently and inspected.

At current densities up to about 30 amp/cm^2, no erosion could be detected for either the water-cooled electrodes or insulators. However, as the current density was increased to 60 amp/cm^2 the insulation between the electrodes began to erode. Since the individual electrodes have a finite length, they provide an equipotential surface over which the Hall potential is locally short-circuited. This gives rise to current concentrations at the downstream edge of the anodes and upstream edges of the cathodes as illustrated by the adjacent simplified sketch. The damage is more severe on the anode side of the channel because the direction of the Lorentz force, F_L, near the electrode surfaces will drive the discharge or current paths into the insulation at the trailing edges of the anode but will pull it away from the cathode leading edges. These current concentrations have been predicted theoretically (see Refs. 15 and 16). They are inherent in the segmented

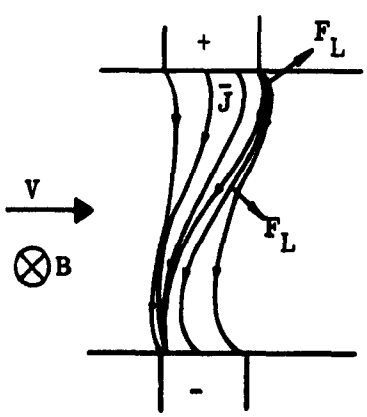

electrode geometry employed in all MHD channels known to the present authors. An approximate analysis in Ref. 15 indicates that when $\omega_e \tau_e = 1$, 50 percent of the current comes from only 8 percent of the electrode surface and such current concentrations become more severe as the value of $\omega\tau$ increases. The $\omega\tau$ for the present accelerator tests was between 1.5 and 2.0. At the moment, it appears that some novel electrode design, perhaps some of those suggested in Ref. 17, may be needed to completely eliminate this problem. However, the insulation erosion is still felt to be tolerable at current densities up to 60 amp/cm^2 (see Fig. 23) and there was no erosion of the copper. In addition, the erosion pattern shown in Fig. 23 demonstrates that the discharge is established almost all across the electrode width after about the fifth powered electrode.

This proof-testing channel was not instrumented as completely as the larger accelerator will be. Electrode voltages and currents were individually measured as were several increments of the Hall voltage. In addition, static pressures in the channel and the impact pressure at the channel exit were obtained.

Although the discharge phenomena adjacent to the electrodes were profoundly altered by application of the magnetic field, the electrode and boundary-layer voltage losses were well predicted by the previous experimental discharge data obtained without a magnetic field. Furthermore, the current-voltage characteristics for the accelerator were nearly identical to those obtained without a magnetic field (for example, Fig. 9) but shifted to a higher voltage level by the amount of the induced voltage.

Typical axial distributions of the electrode current which resulted when a constant electric field was applied to the plasma core are shown in Fig. 24. The current decreases in the downstream portion of the accelerator as would be expected since the Lorentz force increases the gas velocity and hence the induced emf. Using the previous voltage-current discharge data, estimates were made of the additional voltage required in the aft section of the accelerator to achieve a constant current distribution (that is, the E-field was tailored to achieve a constant current density). The results of the first attempt to tailor the fields are also shown in Fig. 24. A reasonably uniform axial current distribution was obtained, and, at least from these preliminary tests, it would appear that tailoring the current to a desired distribution will be no problem in MHD accelerators of this type.

The electrical characteristics in the channel give some evidence of acceleration, but more positive proof is provided by the impact and

static pressure measurements. A time variation of the impact pressure at the accelerator exit during a test is given in Fig. 25. Various operating events are also indicated in this plot. The impact pressure rises abruptly when current begins to flow across the channel at t = 4.7 sec; when the current was interrupted at t = 12.3 sec, the impact pressure returned to its original value. Also, during this time the static pressure in the aft portion of the channel was observed to decrease slightly. Since the flow is supersonic and the duct area essentially constant, the rise of impact pressure only occurs if the plasma is being accelerated; hence, it is an index indicating the amount of acceleration. Carter, et al. (Ref. 2) discuss this in more detail.

The increases of impact pressure obtained during the tests with this channel are shown in Fig. 26 for various operating conditions. Up to 65-percent increases of the impact pressure have been obtained, and the channel has been operated at current densities to 60 amp/cm^2. Both the pressure and electrical measurements independently indicate that this channel has produced a 25- to 30-percent increase in the plasma velocity. No attempt was made to make a direct velocity measurement. The impact pressure rises and velocity increases achieved are somewhat greater than predicted by the theoretical calculations. Based on these test results it appears that the larger accelerator described in Section 7.0 will at least produce a velocity ratio in excess of 2.

The sketch of the current paths presented previously in this section illustrates that the Lorentz force is not acting in the axial direction. Some preliminary tests were also made to determine if the acceleration could be improved by shifting the anodes upstream, thus creating an axial component of the applied E-field to make the current flow straight across the channel. (Actually, cathode 8 was electrically connected to anode 7 and so on down the channel). When the differences in seeding rate, wall roughness, etc., were taken into account, shifting the anodes appears to produce a somewhat larger velocity increase. A nearly direct comparison is shown in Fig. 26 by the two filled-in symbols. Figure 26 also demonstrates the benefit of keeping the conductivity high. As the seeding rate and presumably the plasma conductivity decrease, the impact-pressure rise decreases quite significantly. This occurs because a larger portion of the input power goes into ohmic heating, and the accelerator is thus operating less efficiently.

A typical axial distribution of the Hall potentials developed in the channel is shown in Fig. 27. Since the front end of the channel was at ground potential, the generated Hall field drove the aft end of the device to large negative voltages with respect to ground. Axial potentials up to about 27 v per electrode were developed in these tests, and the maximum

Hall field achieved was 4100 v/m. Both the electrode and sidewall insulation performed well under these conditions. The sidewalls in this channel were identical to each section of the sidewall which will be used in the larger accelerator. They were operated at the same conditions at which each section of the segmented sidewall will operate in the accelerator described in Section 7.0. However, the problem of isolating the 1500-v Hall potential from ground for this larger accelerator must be solved.

The 20-electrode proof-test accelerator has operated at its design conditions, and, in general, its performance has been satisfactory. The only unexpected problem which is not yet completely resolved again centers about the seed material. The $K_2CO_3 + H_2O$ seed penetrates the BeO coating. It not only tends to reduce the resistance between parts in the channel but reacts chemically with the copper and BeO at their interface and tends to loosen the bond. At the present, ways are being explored to eliminate this problem as well as a somewhat modified electrode design in an attempt to decrease the insulation erosion between electrodes.

9.0 CONCLUDING REMARKS

The accelerator development program at AEDC is still in progress and to date much has been learned about the construction and operation of a steady-flow JxB accelerator which would operate at near atmospheric pressure with a seeded plasma. The progress made has been quite encouraging, and no insurmountable problems have been encountered. However, the work has not as yet advanced to the state where an accelerator could be used for routine wind tunnel testing. Acceleration of a plasma at near atmospheric pressure has been demonstrated with a small proof-testing channel, and a larger accelerator has been constructed which should at least double the plasma velocity. It will be tested in the near future. The most important problem which must be solved centers about the more effective use of the seeding material. Also, all operations to date have utilized a non-oxidizing test medium (nitrogen). Acceleration of air will be undertaken in the immediate future.

REFERENCES

1. Ring, L. E. "General Considerations of MHD Accelerators for Aerodynamic Testing." AEDC-TDR-64-256, to be published.
2. Carter, Arlen F., et al. "Experiments in Steady-State High-Density Plasma Acceleration." Proceedings of the Second Symposium on the Engineering Aspects of Magnetohydrodynamics, University of Pennsylvania, March 9-10, 1961.
3. Hogan, W. T. "An Experimental Investigation of a Magneto-gasdynamic Accelerator." Magnetogasdynamics Laboratory Report No. 62-1, M.I.T., January 1962.
4. Demetriades, S. T. and Ziemer, R. W. "Three Fluid Non-Equilibrium Plasma Accelerators." Presented at the American Rocket Society Electric Propulsion Conference, Paper No. 2375-62, March 14-16, 1962.
5. Louis, J. F., Lothrop, J., and Brogan, T. R. "Fluid Dynamic Studies with a Magnetohydrodynamic Generator." The Physics of Fluids, Vol. 7, No. 1, March 1964, p. 362.
6. Wood, G. P., et al. "Research on Linear Crossed-Field Steady-Flow DC Accelerators at Langley Research Center, NASA." Presented at the AGARD Specialists' Meeting on Arc Heaters and MHD Accelerators for Aerodynamic Purposes, Rhode-Saint-Genese, Belgium, September 21-23, 1964.
7. Wagoner, C. B. Private Communication, October 1963.
8. Wilson, D. R., Clouse, C. E., and Schaetzle, W. J. "Development of a Computer Program for the Analysis of One-Dimensional Magnetohydrodynamic Flow Problems." AEDC-TDR-63-45 (AD403793L), January 1964.
9. Tempelmeyer, K. E., Whoric, J. M., Rittenhouse, L. E., and McKee, M. L. "Some Characteristics of an Electrical Discharge Transverse to a Supersonic Seeded Nitrogen Plasma Stream with Cold Copper Electrodes." AEDC-TDR-64-231, to be published.
10. Dicks, John B. "Improvements in Design of MHD Accelerator Channels for Aerodynamic Purposes." Presented at the AGARD Specialists' Meeting on Arc Heaters and MHD Accelerators for Aerodynamic Purposes, Rhode-Saint-Genese, Belgium, September 21-23, 1964.

11. Weber, R. E. and Tempelmeyer, K. E. "Calculation of the D-C Electrical Conductivity of Equilibrium Nitrogen and Argon Plasma with and without Alkali Metal Seed." AEDC-TDR-64-119 (AD602858), June 1964.

12. Kerrebrock, Jack L. "Conduction in Gases with Elevated Electron Temperature." Proceedings of the Second Symposium on the Engineering Aspects of Magnetohydrodynamics, University of Pennsylvania, March 9-10, 1961.

13. Kerrebrock, J. L. and Hoffman, M. A. "Experiments on Non-Equilibrium Ionization Due to Electron Heating." Presented at the 1964 AIAA Aerospace Sciences Meeting, Preprint 64-27, New York, N. Y., January 20-22, 1964.

14. Zukowski, E. E., Cool, T. A., and Gibson, E. G. "Experiments Concerning Non-Equilibrium Conductivity in a Seeded Plasma." Presented at the 1964 AIAA Aerospace Sciences Meeting, Preprint 64-28, New York, N. Y., January 20-22, 1964.

15. Hurwitz, H., Jr. Kilb, R. W., and Sutton, G. W. "Influence of Tensor Conductivity on Current Distribution in a MHD Generator." Journal of Applied Physics, Vol. 32, No. 2, February 1961, pp. 205-216.

16. Crown, J. Conrad. "Analysis of Magnetogasdynamic Generators Having Segmented Electrodes and Anisotropic Conductivity." United Aircraft Report R-1852-2, February 1961.

17. Sutton, G. W. "Theoretical Performance of MHD Generators with Various Electrode Geometries." Proceedings of Fifth Symposium on the Engineering Aspects of Magnetohydrodynamics, M.I.T., April 1-2, 1964, pp. 61.

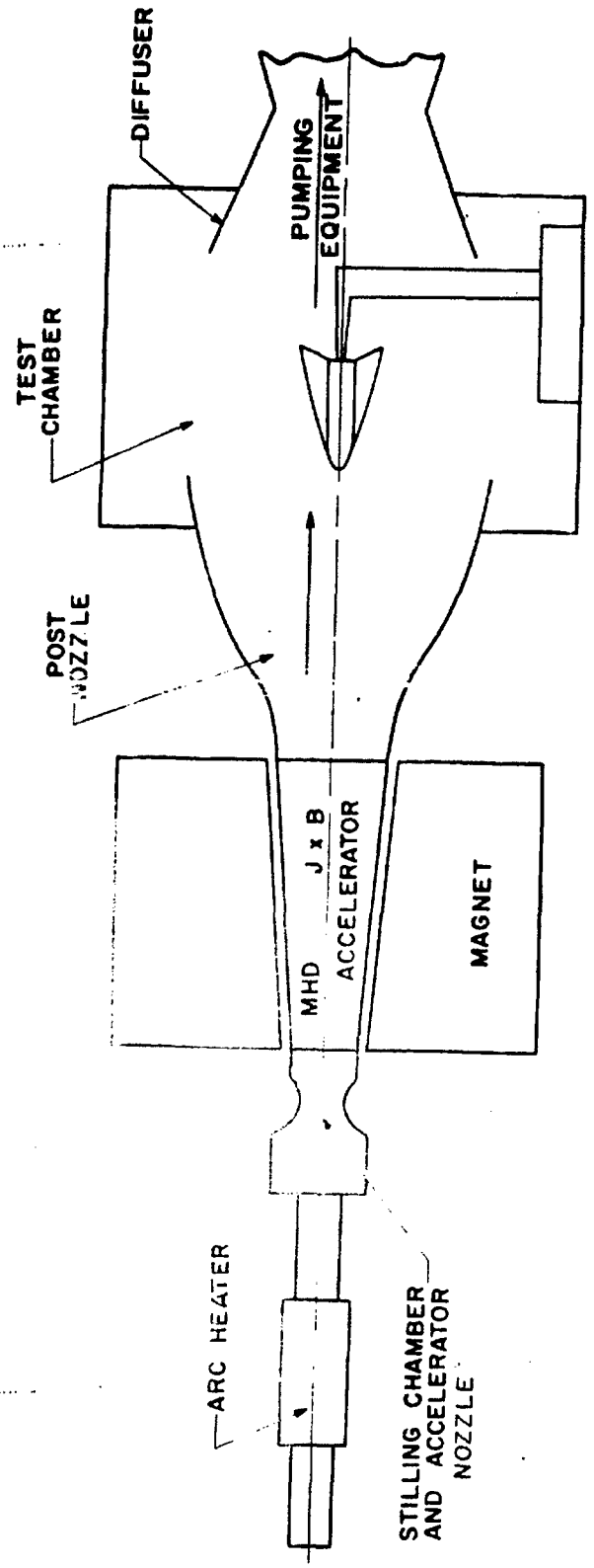

Fig. 1 AEDC Concept of a MHD-Powered Hypersonic Test Facility

Preceding Page Blank

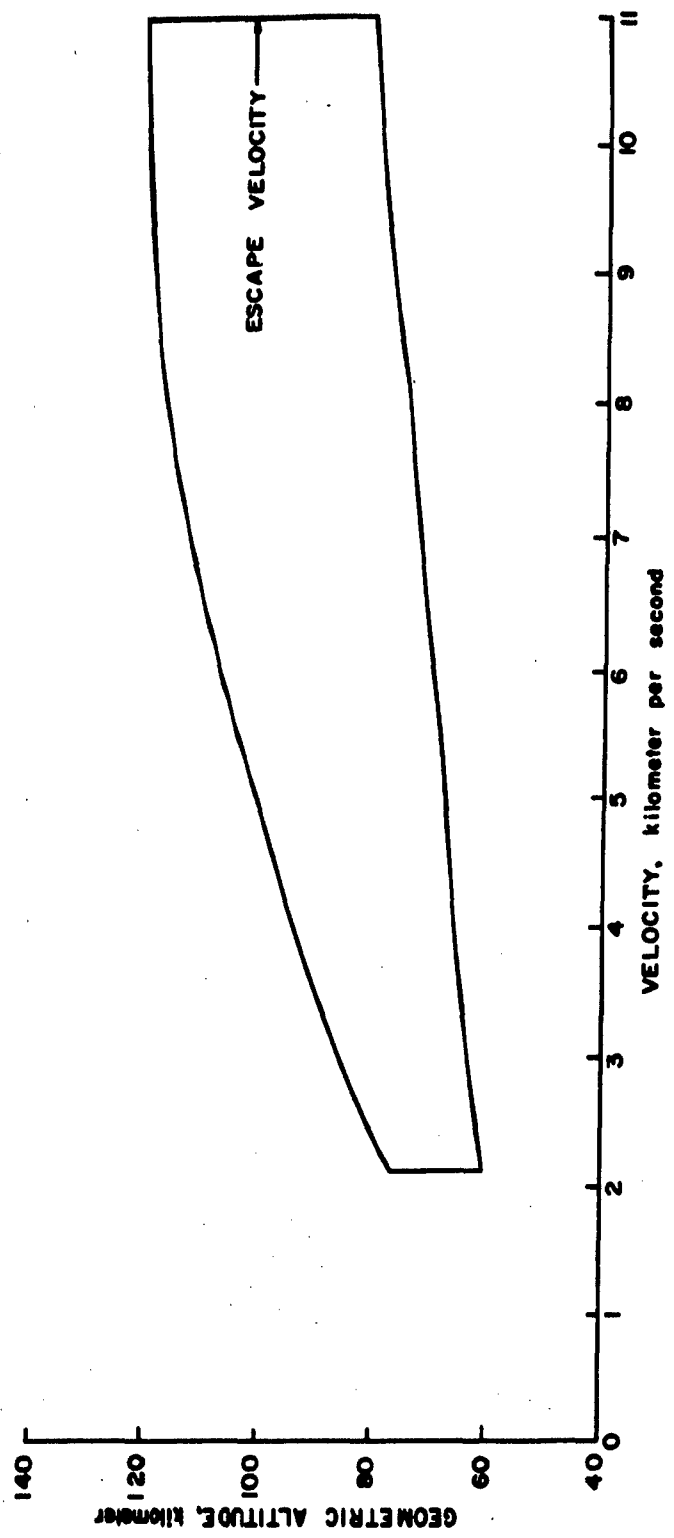

Fig. 2 Desired Altitude Velocity Range

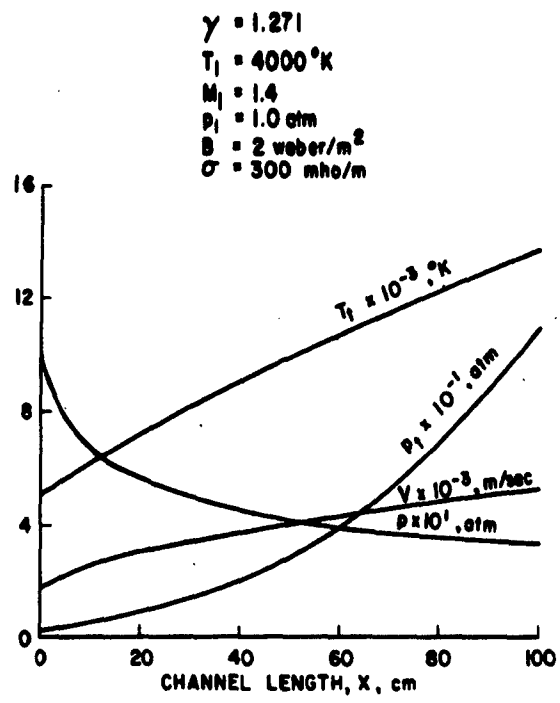

a. Gas Dynamic Characteristics

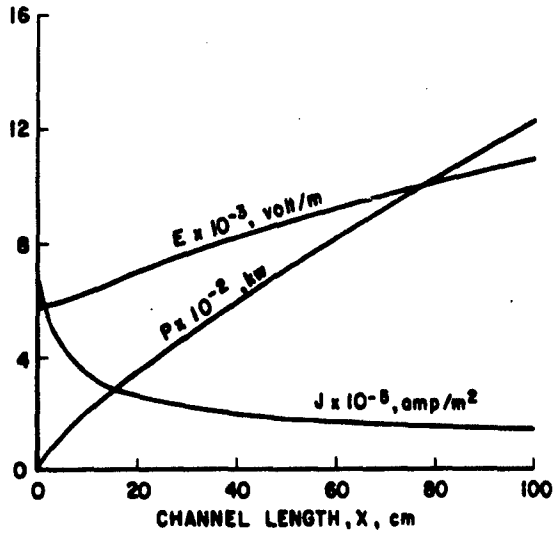

b. Electrical Characteristics

Fig. 3 Typical MHD Accelerator Operating Conditions

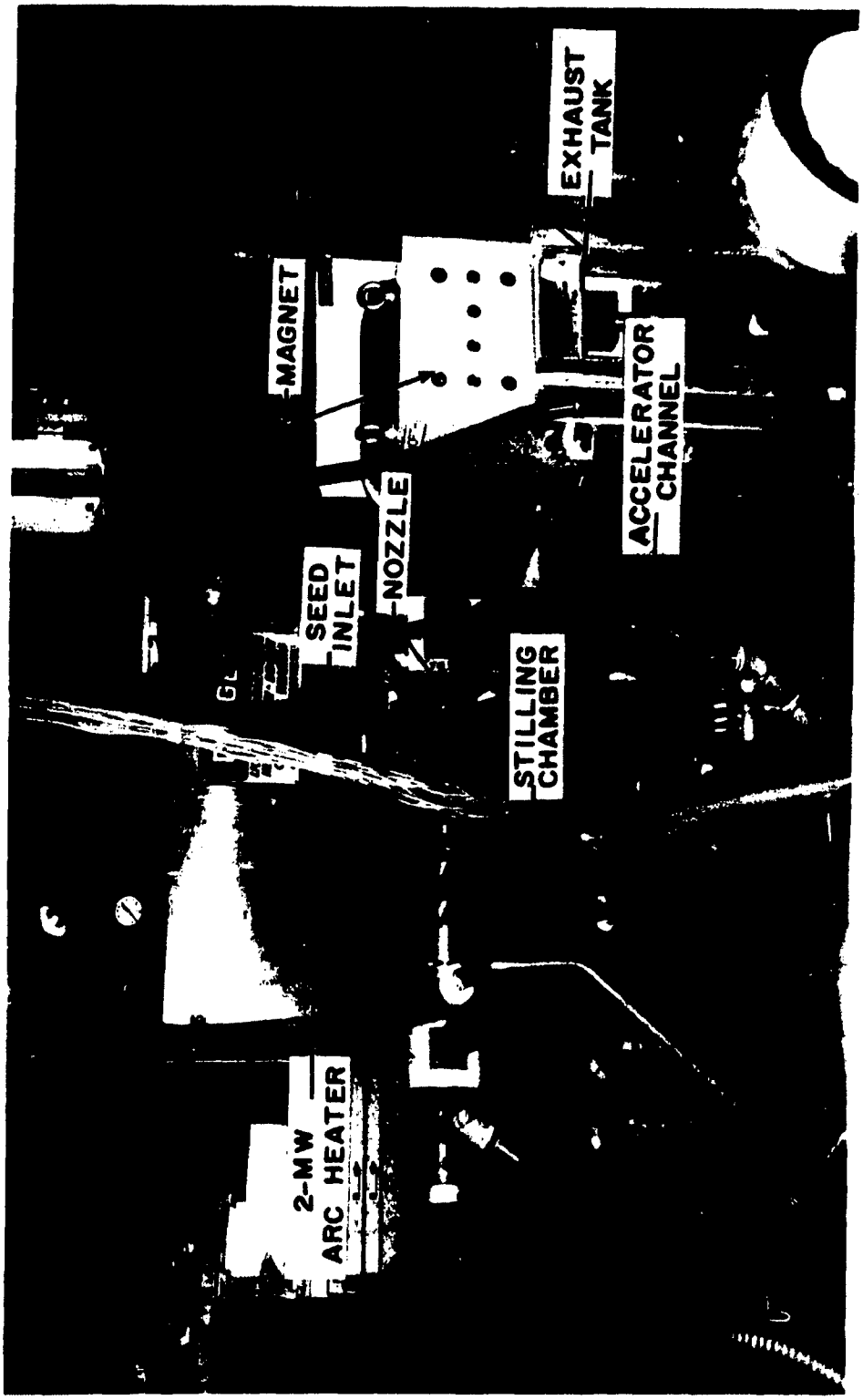

Fig. 4 Test Apparatus

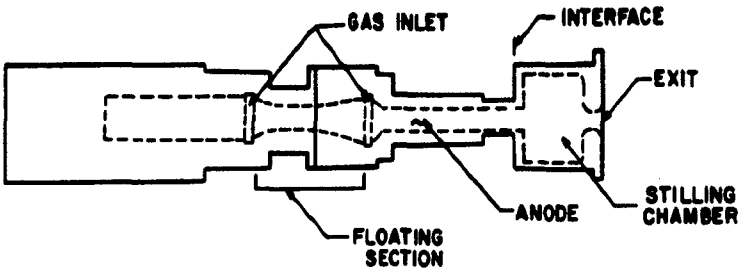

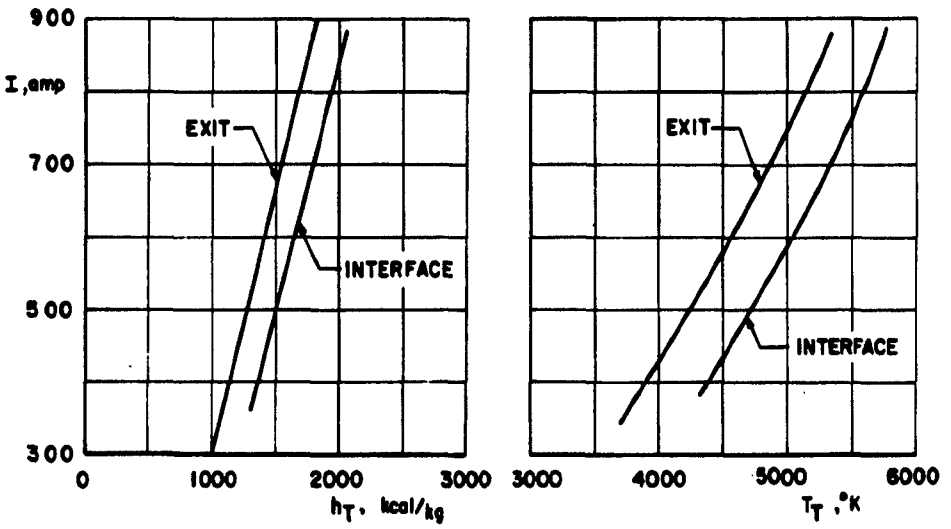

W_g = 0.091 kg/sec

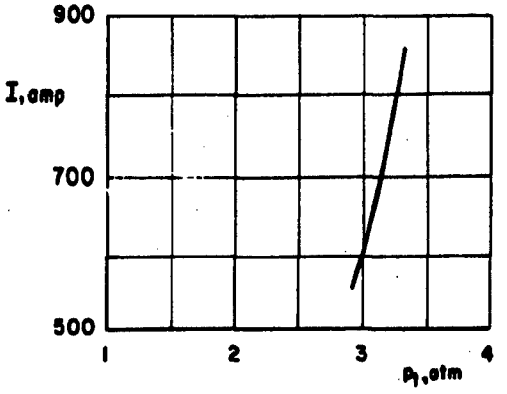

Fig. 5 Typical Arc-Heater Performance Characteristics

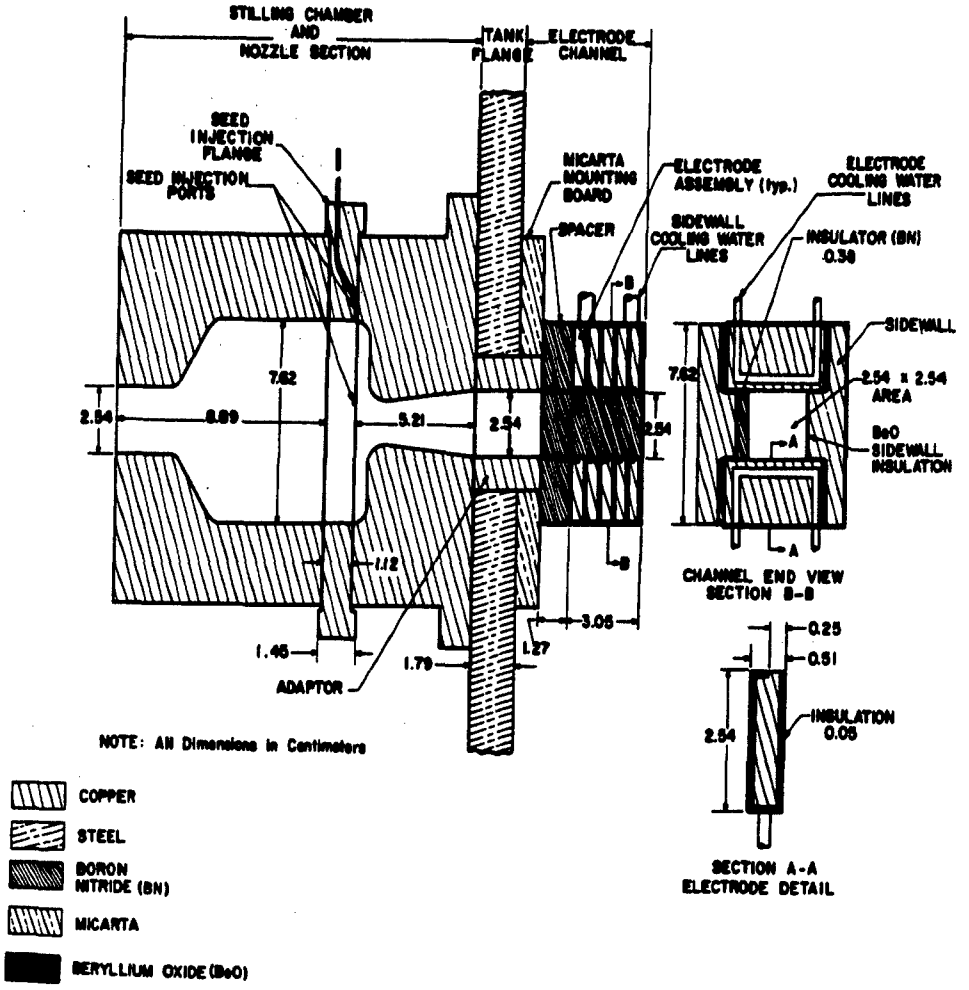

a. Beryllia Insulation between Electrodes

Fig. 6 Electrical Discharge Test Channels

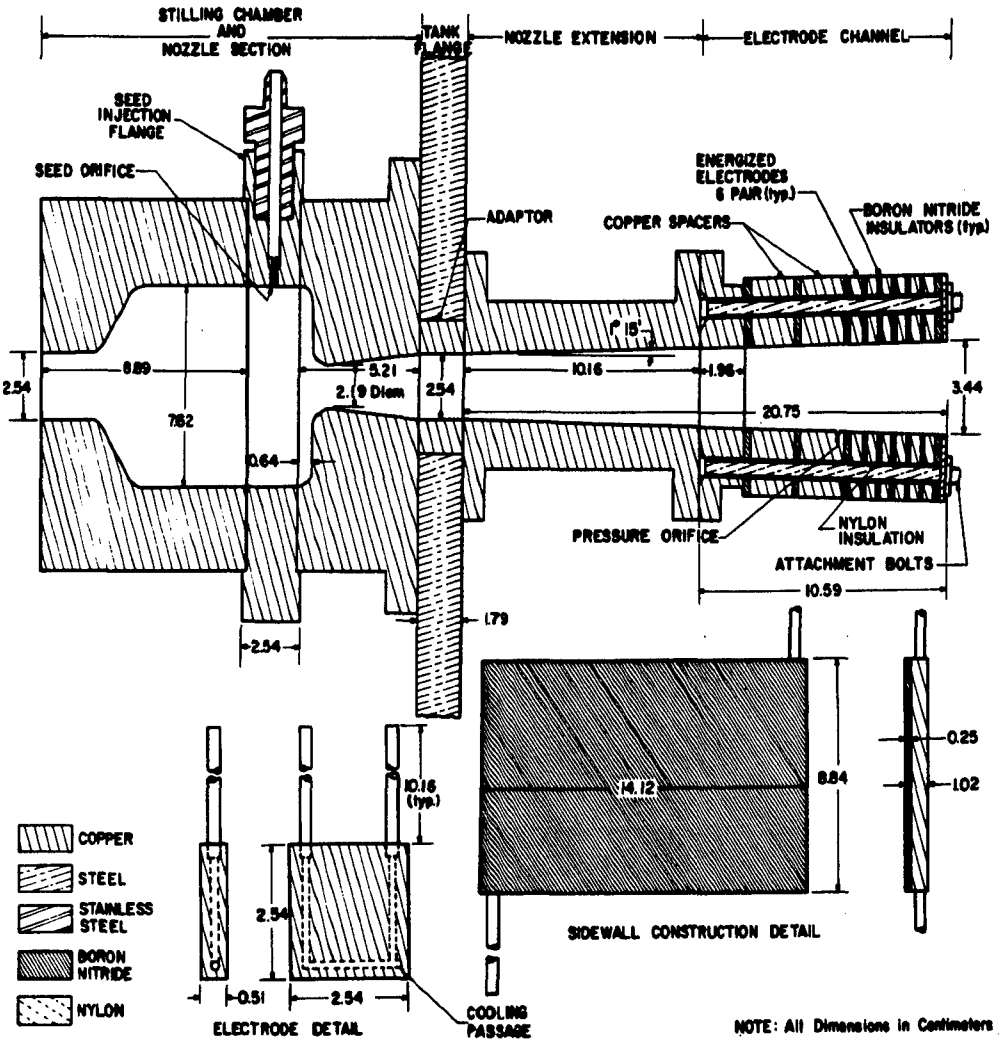

b. Boron Nitride Insulation between Electrodes

Fig. 6 Concluded

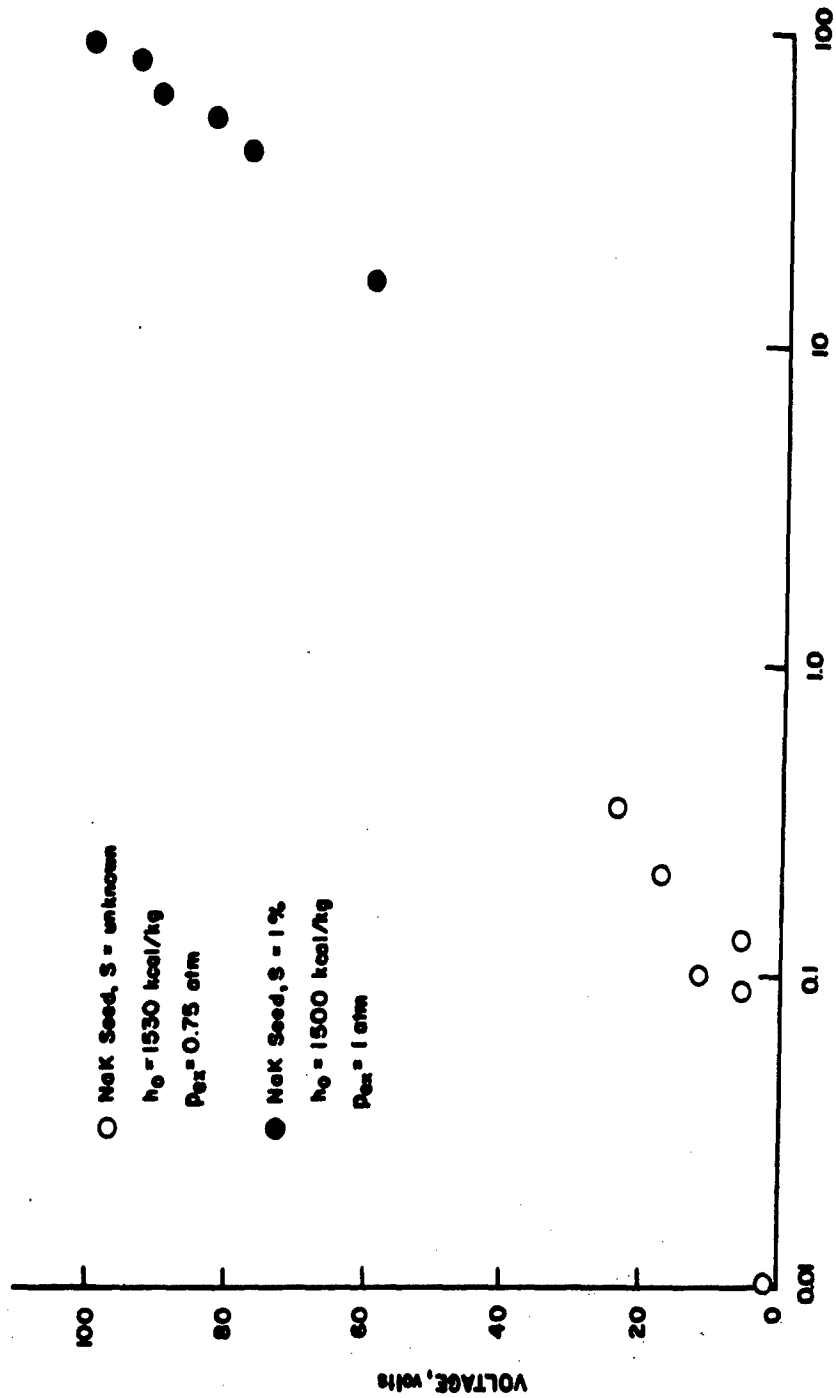

Fig. 7 Current-Voltage Characteristics over a Large Current Range

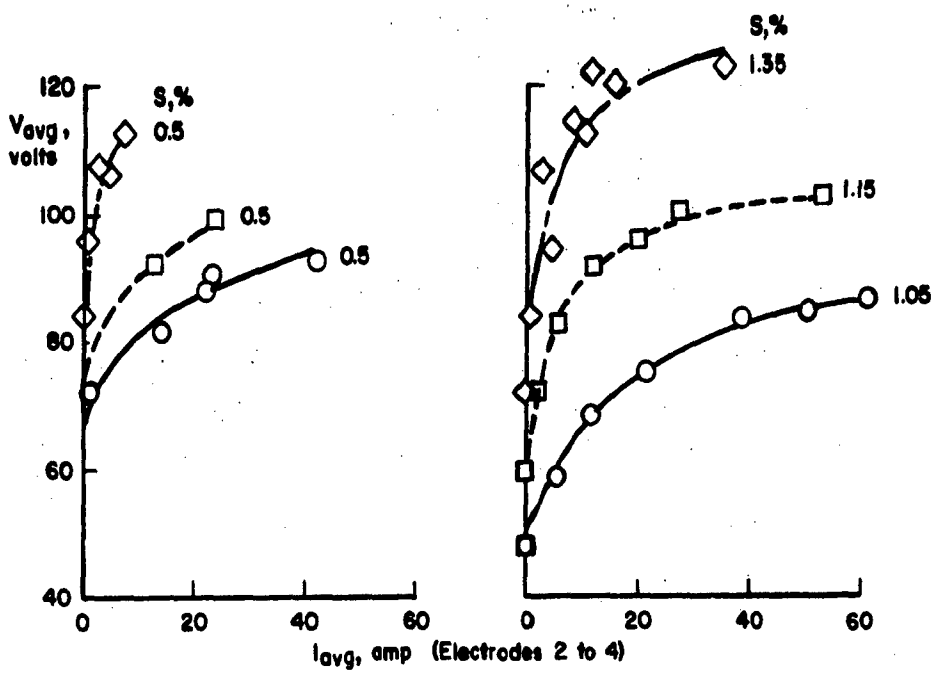

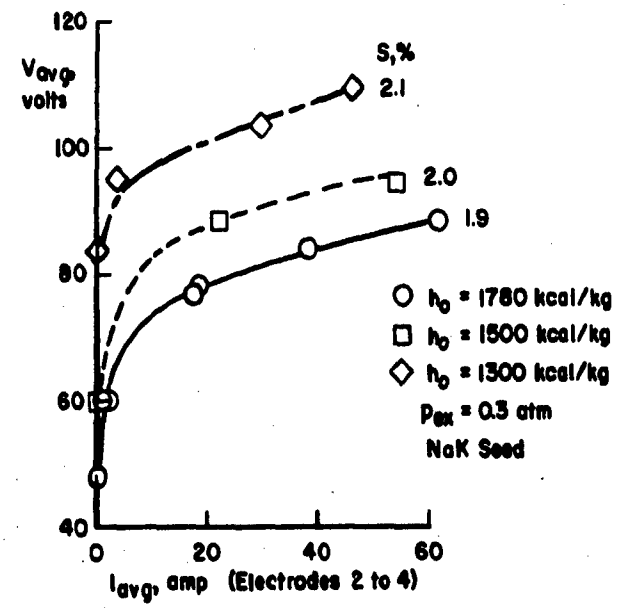

Fig. 8 Average Current-Voltage Characteristics at Various Seed Rates and Enthalpy Levels

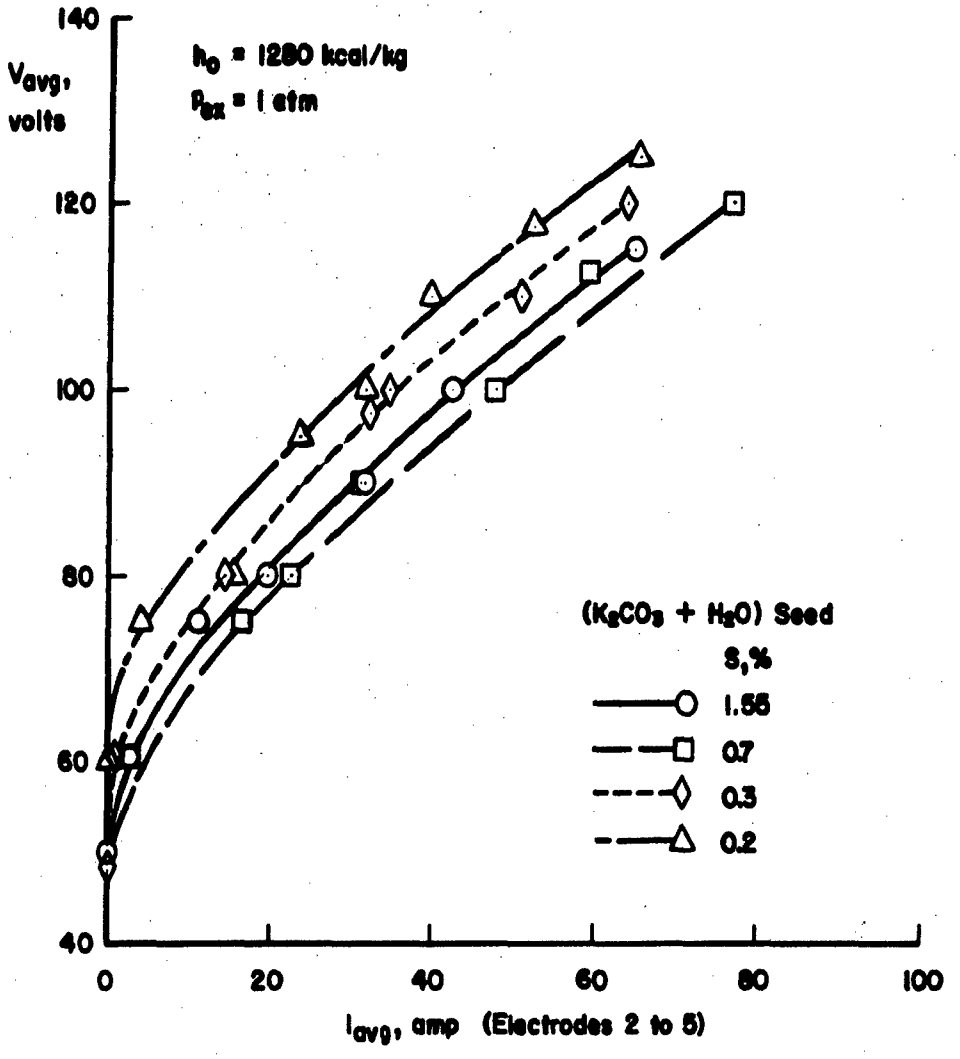

Fig. 9 Averaged Current-Voltage Characteristics at Various K_2CO_3 + H_2O Seed Rates

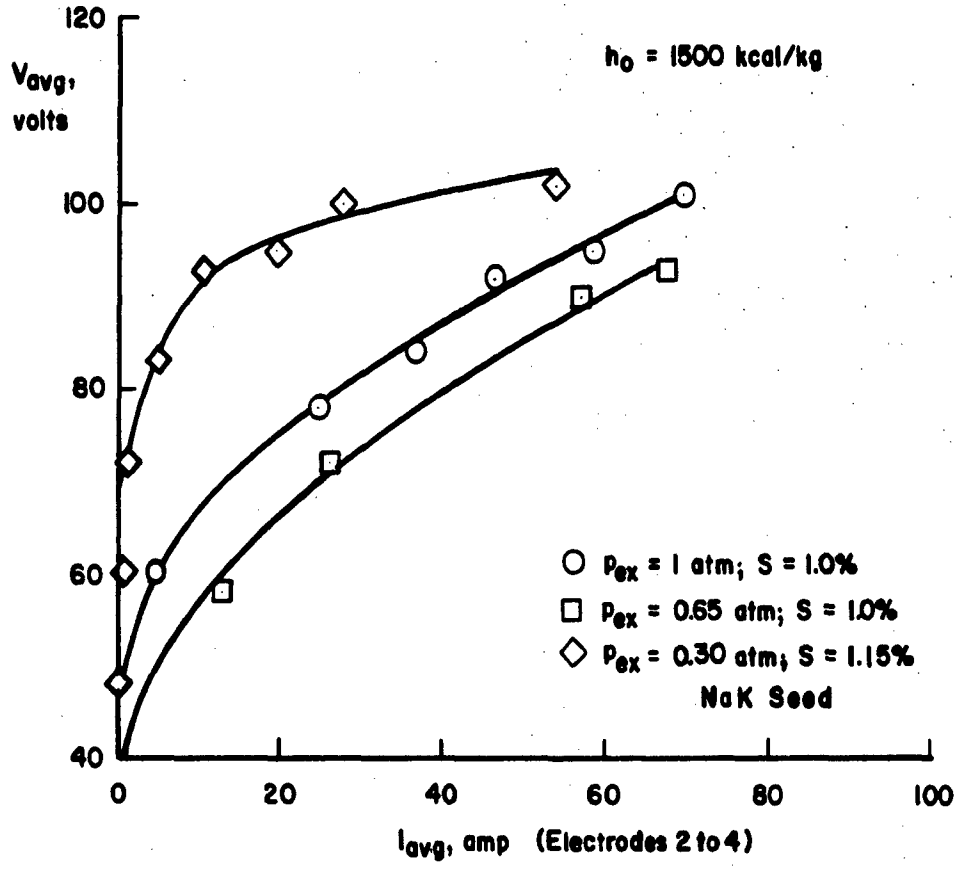

Fig. 10 Averaged Current-Voltage Characteristics at Various Pressure Levels

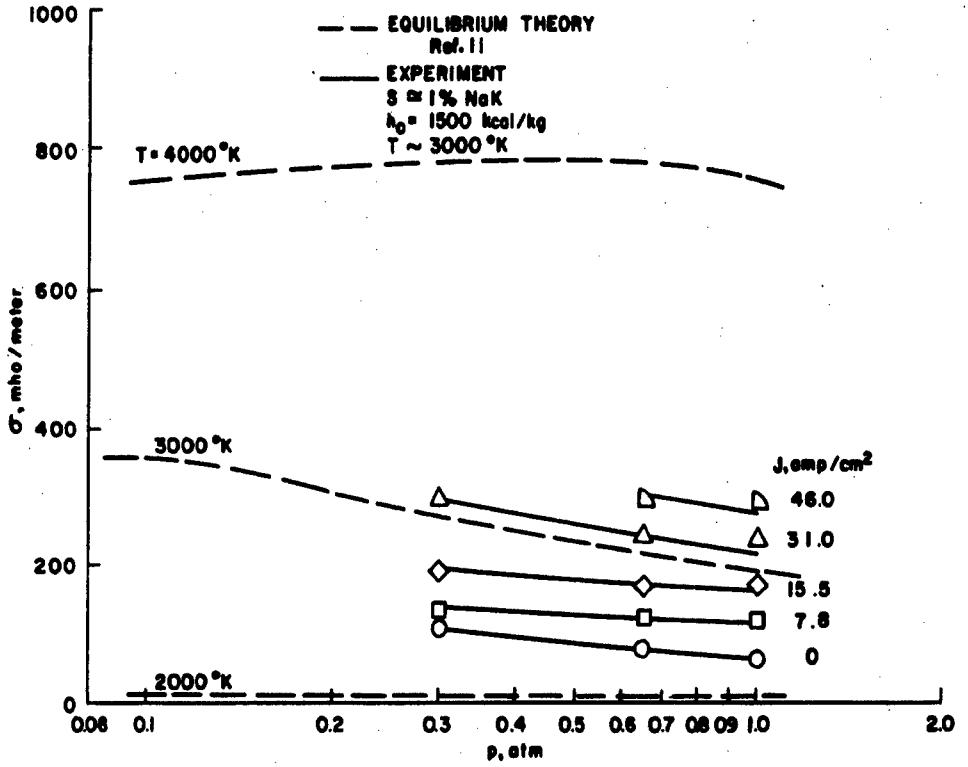

Fig. 11 Electrical Conductivities with NaK Seeding

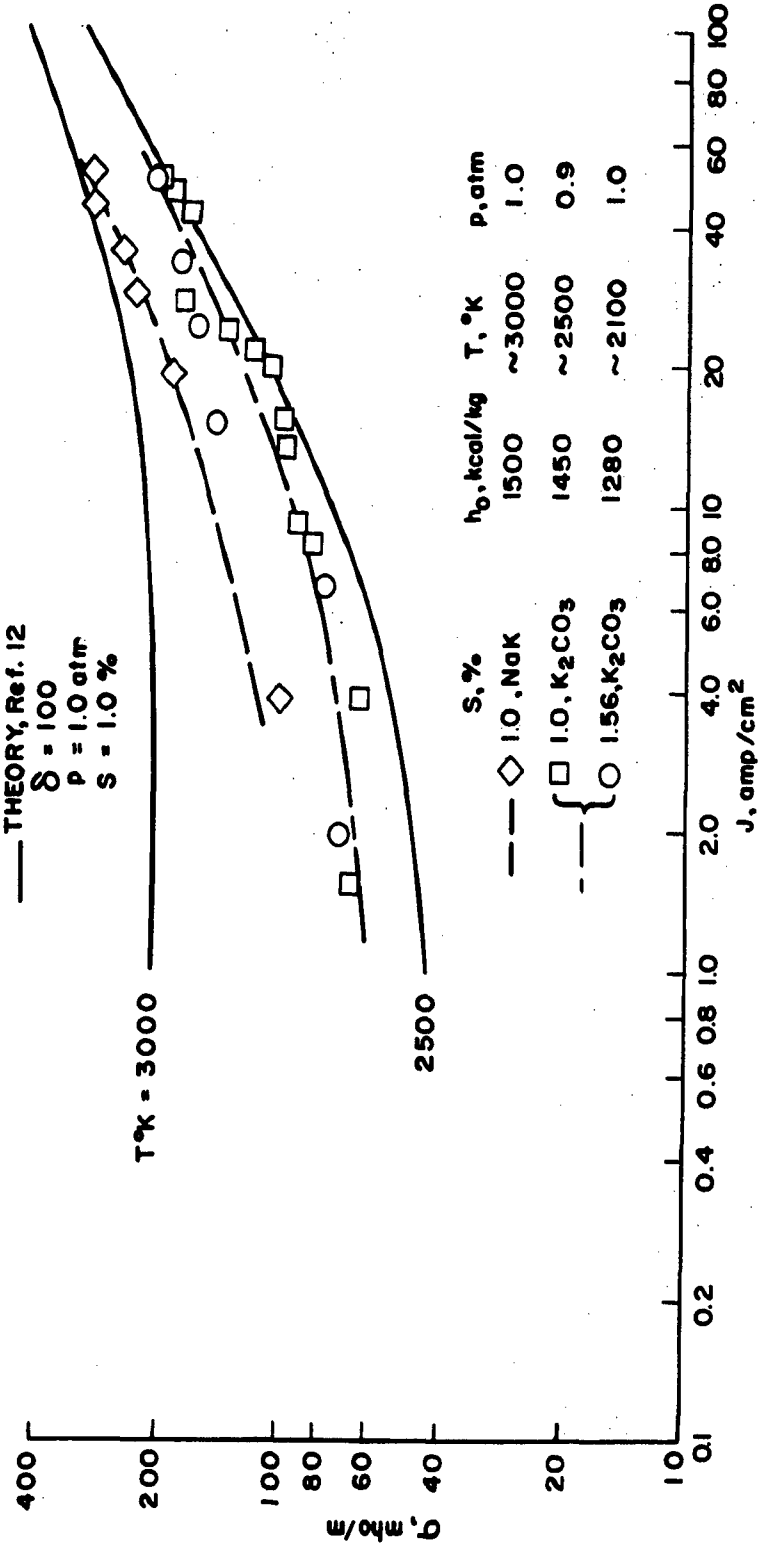

Fig. 12 Comparison of Electrical Conductivity with Nonequilibrium Electron Temperature Theory

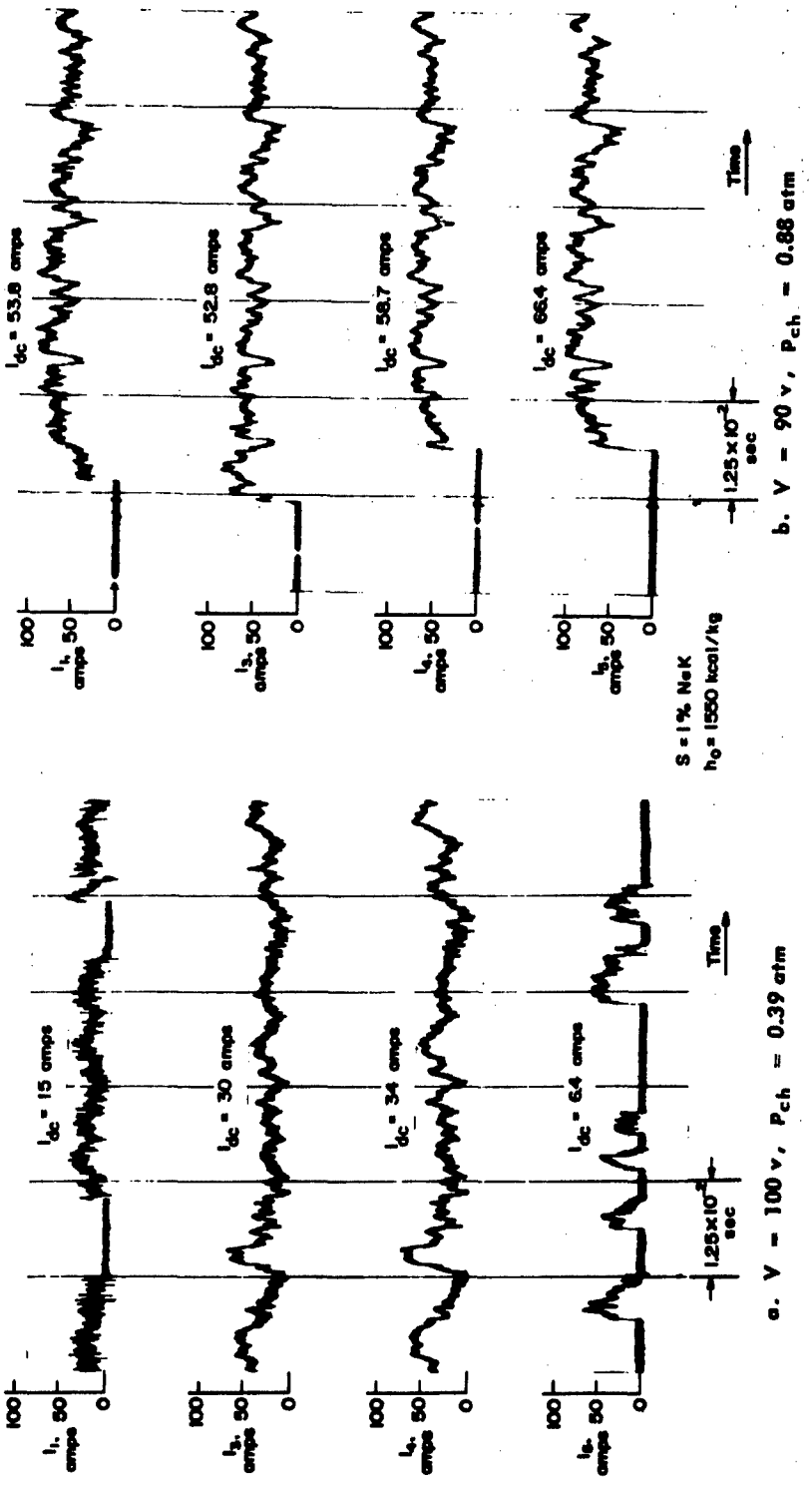

Fig. 13 High-Frequency Current Fluctuations

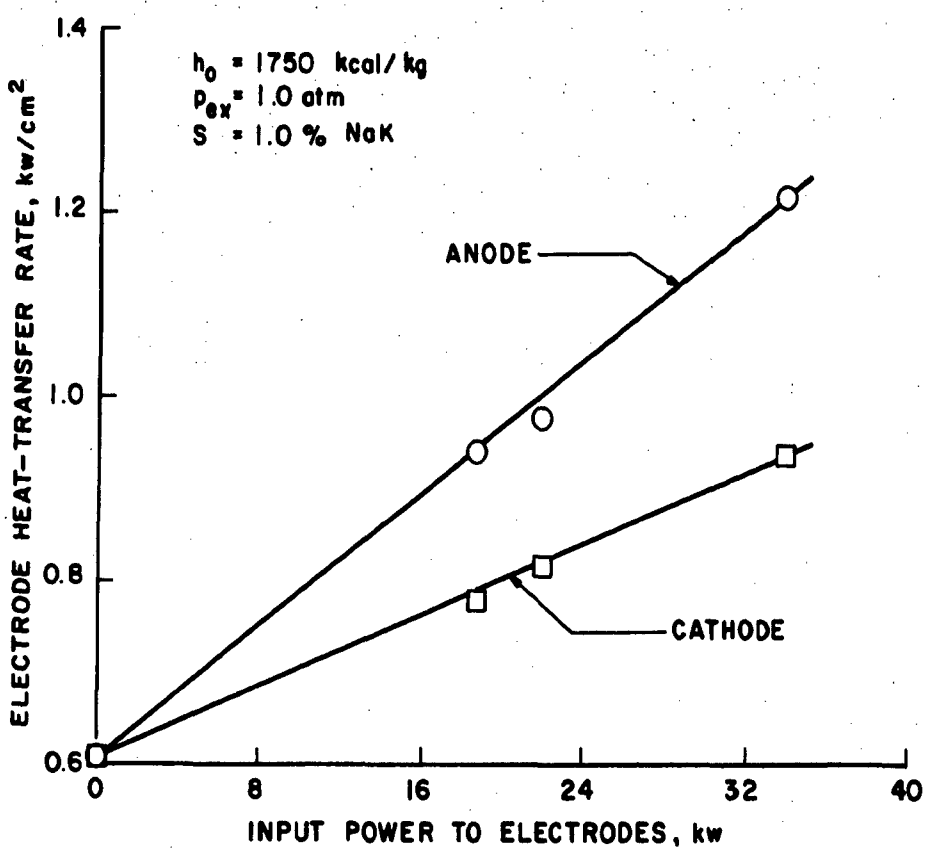

Fig. 14 Electrode Heat-Transfer Rates

Fig. 15 Erosion of Water-Cooled Copper Electrodes

C-1, 2, 4, 6 UNCOOLED TUNGSTEN
C-3, 5 COOLED COPPER

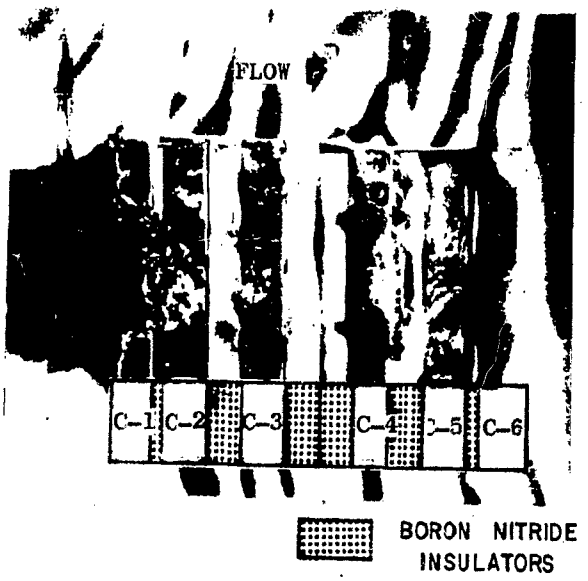

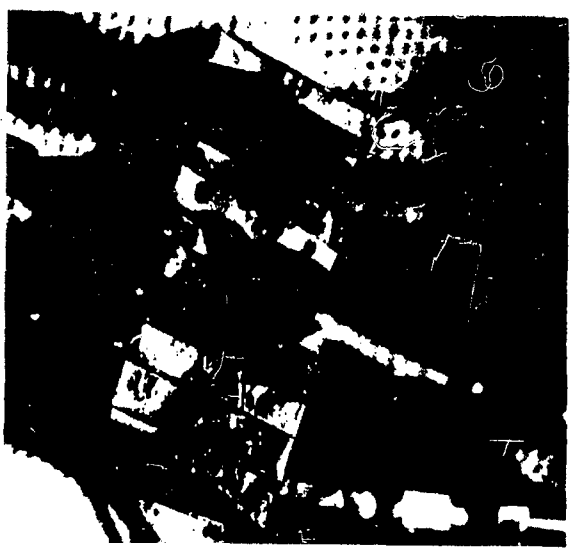

CATHODES AND INSULATORS AFTER POINT 20

Fig. 16 Erosion on Uncooled Tungsten Electrodes

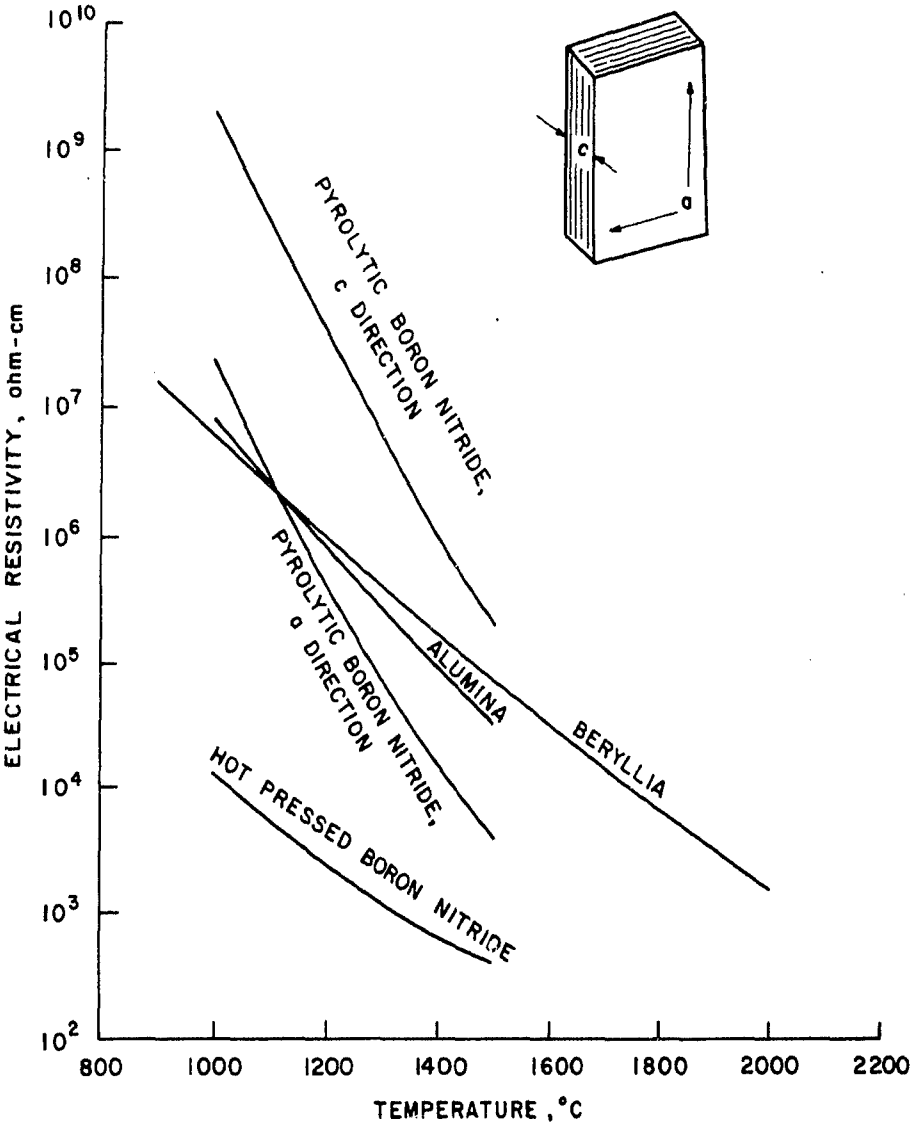

Fig. 17 Electrical Resistivity of Several High-Temperature Insulators

a. Boron Nitride Insulation

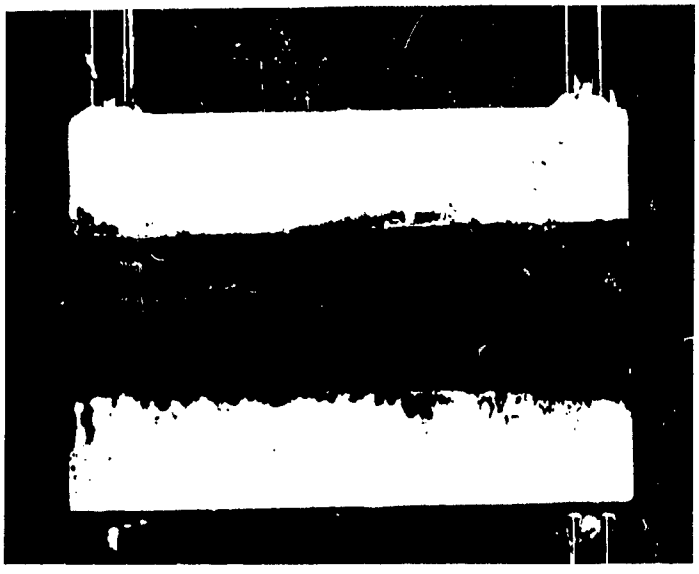

b. Sprayed Beryllia Insulation

Fig. 18 Insulated Sidewalls after Tests

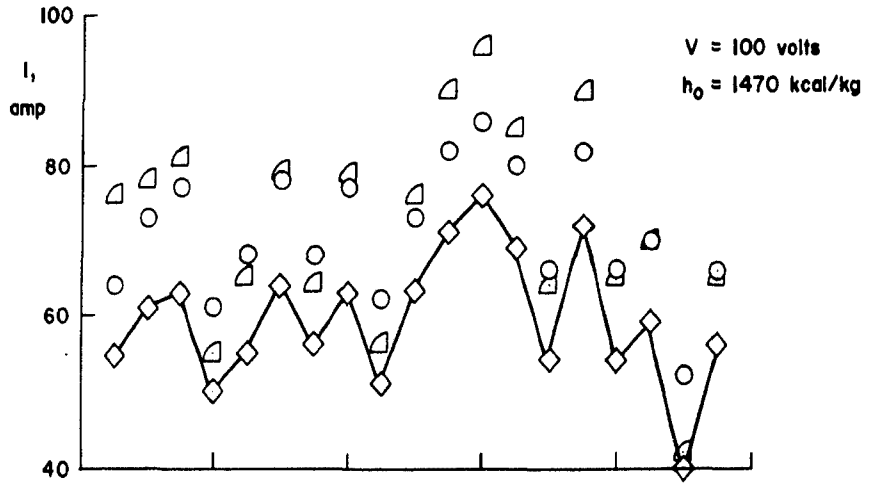

a. K_2CO_3 Powder Seed, S = 1 percent

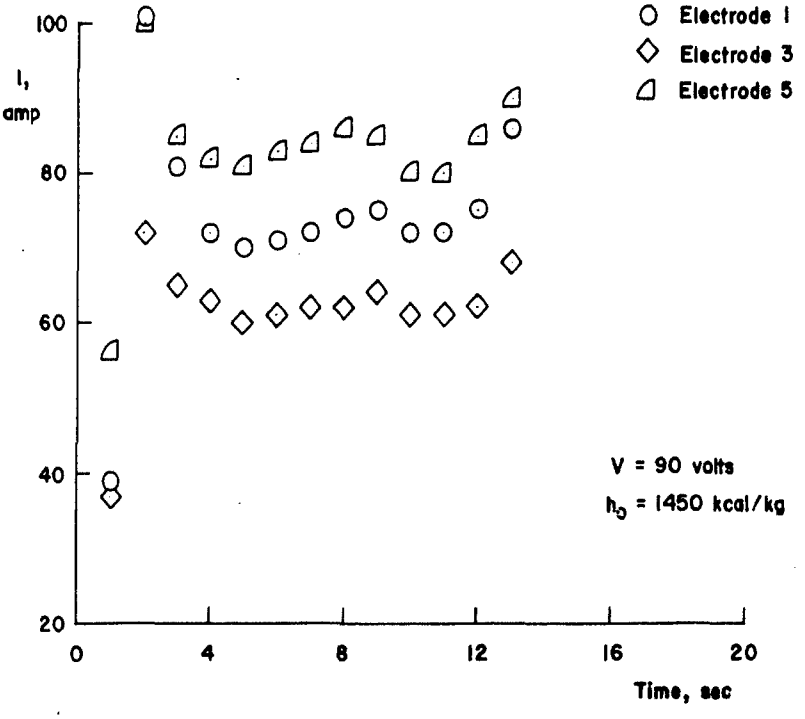

b. (K_2CO_3 + H_2O) Seed, S = 1.05 percent

Fig. 19 Long-Duration Current Fluctuations with K_2CO_3 Seed

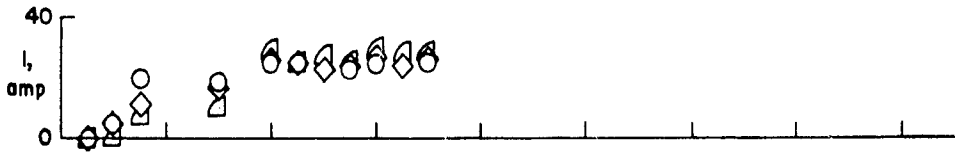

a. S = 0.5 percent, NaK Seed

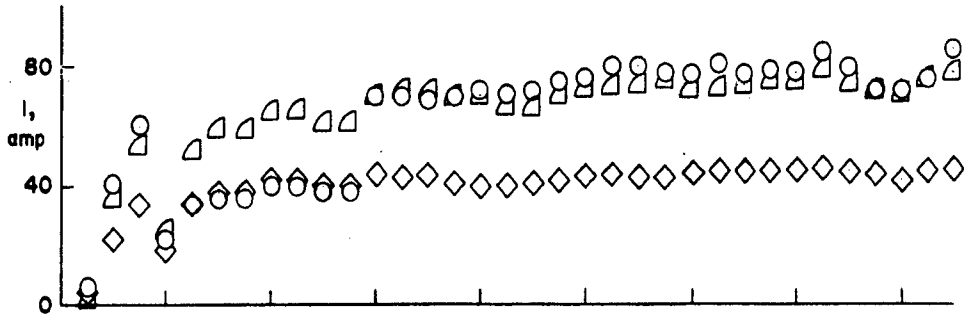

b. S = 1.05 percent, NaK Seed

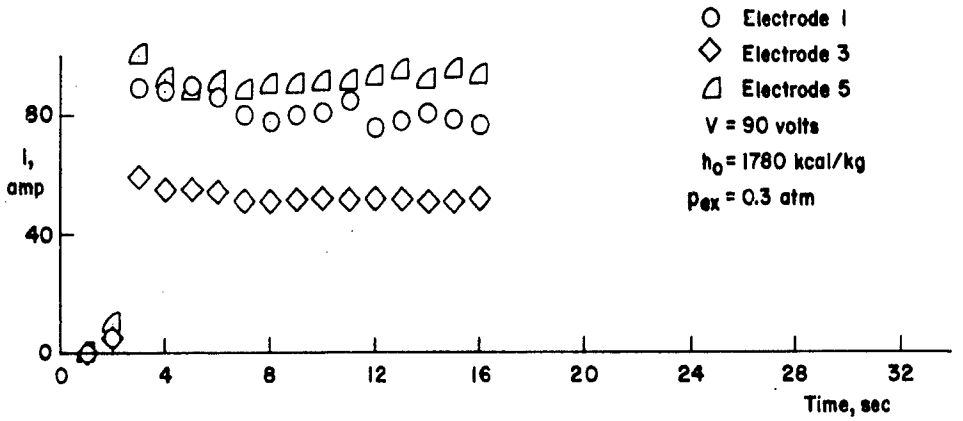

c. S = 1.9 percent, NaK Seed

Fig. 20 Long-Duration Current Fluctuations with NaK Seed

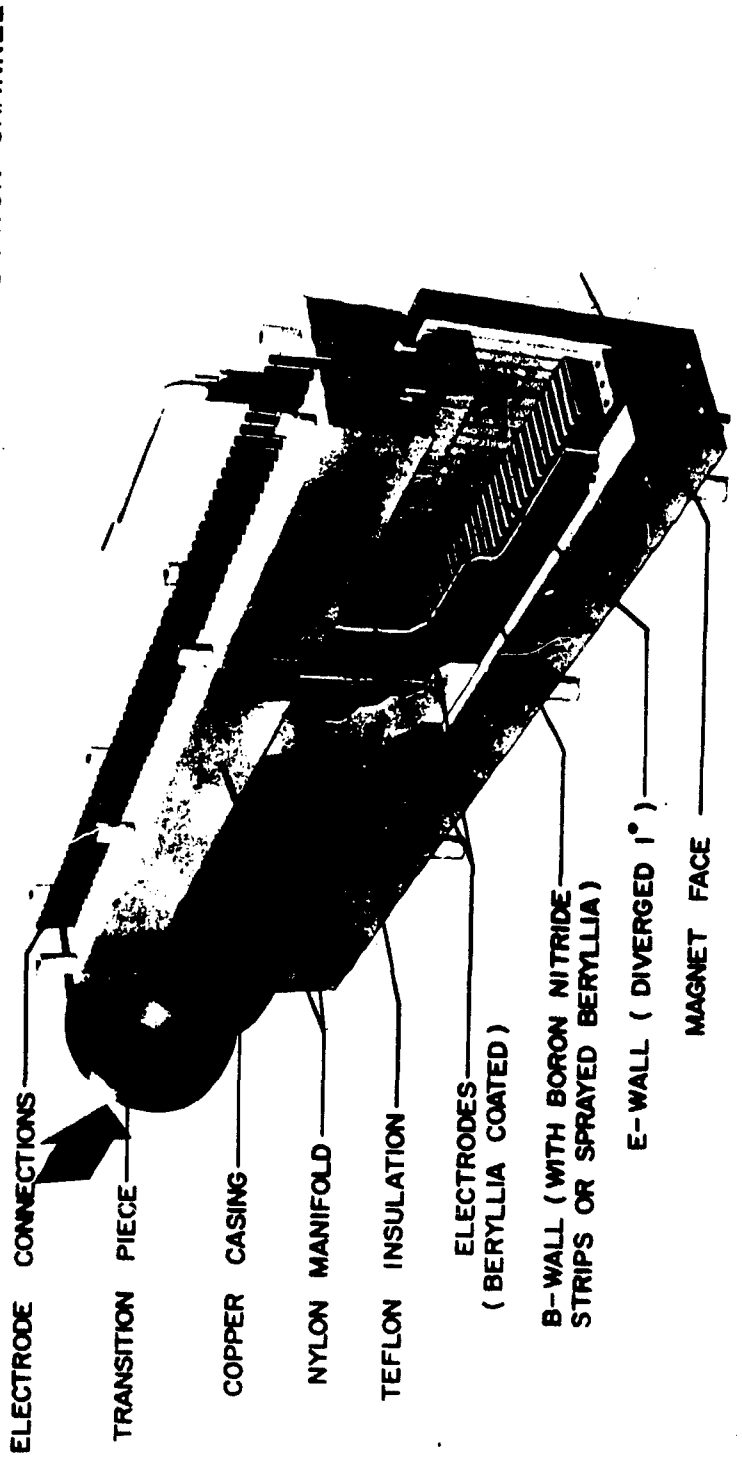

Fig. 21 Accelerator Design – Artist Concept

Fig. 22 Twenty-Electrode Accelerator with One Sidewall Removed

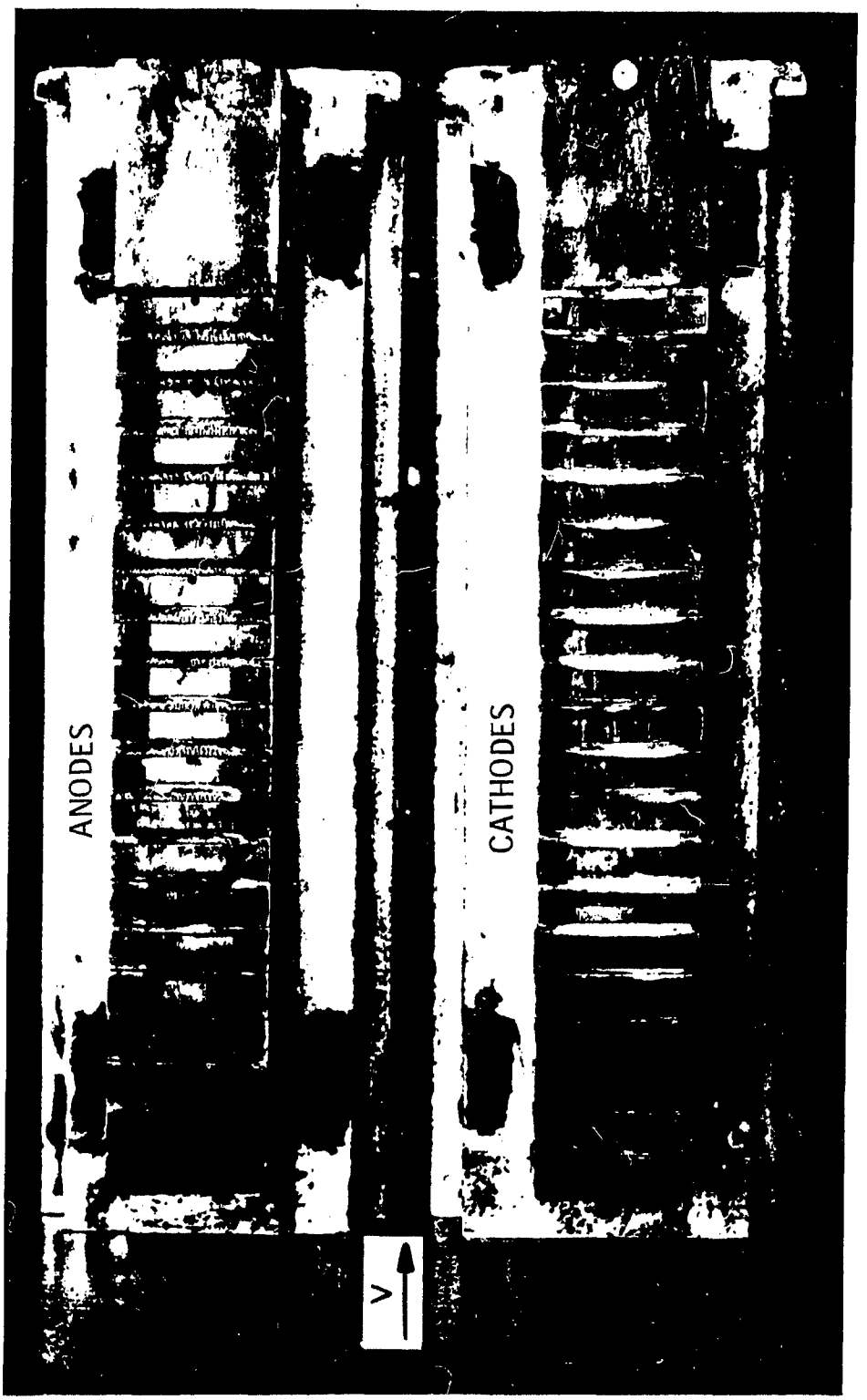

Fig. 23 Twenty-Electrode Accelerator Electrode Wall after Approximately Three Minutes of Powered Operation

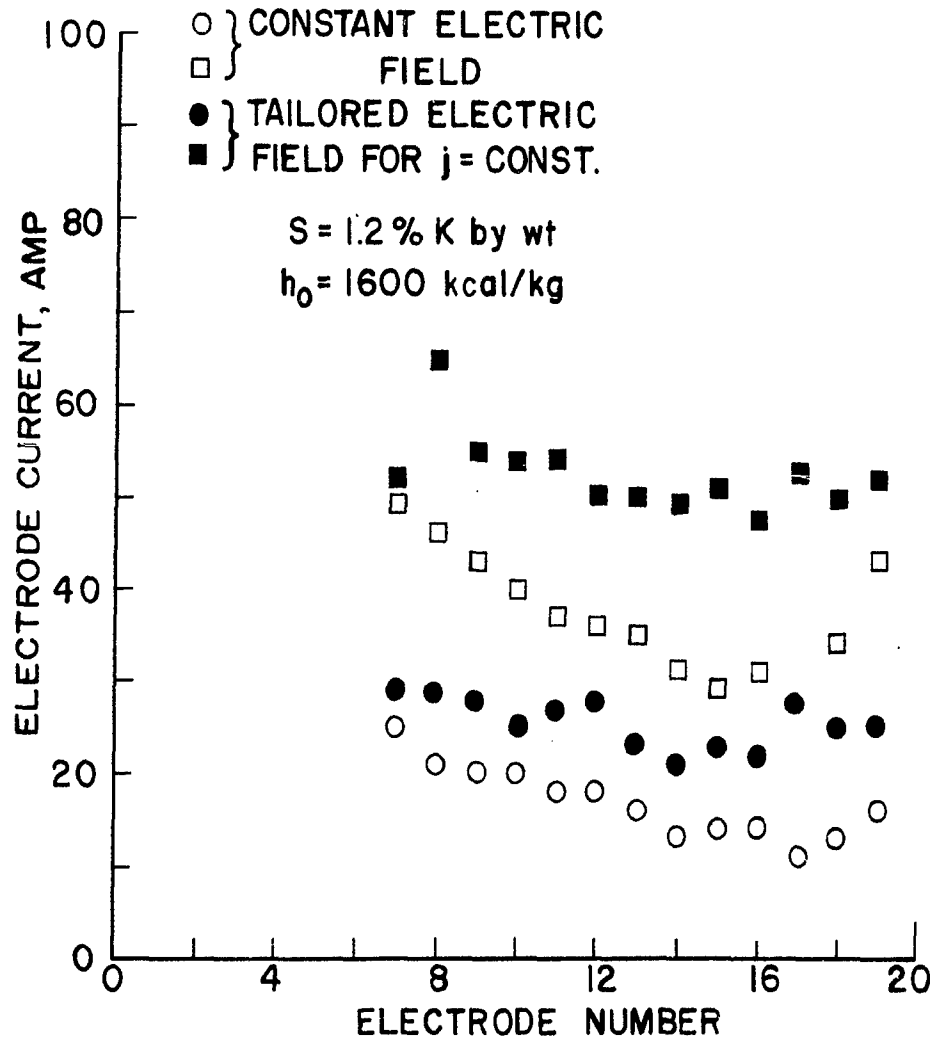

Fig. 24 Typical Current Distributions in 20-Electrode Proof-Test Channel

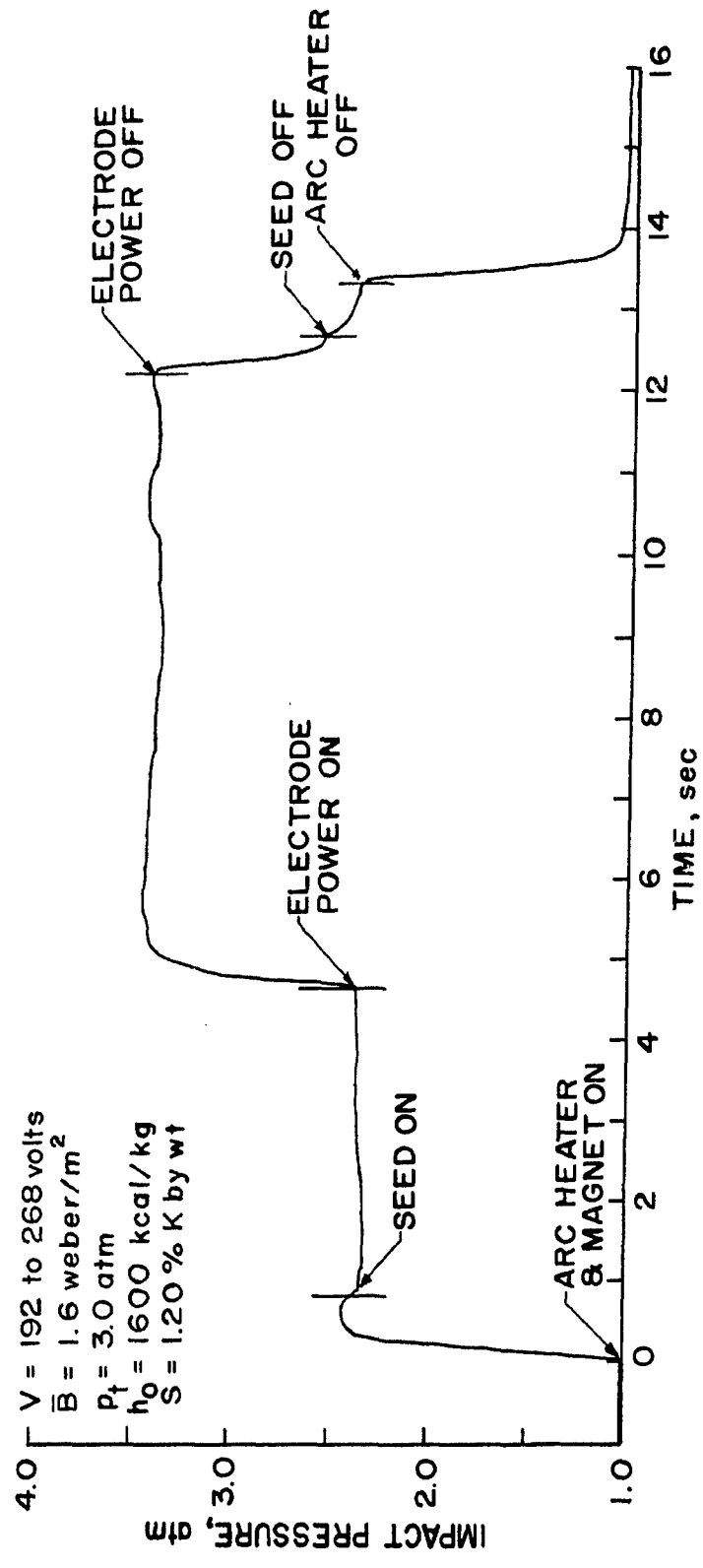

Fig. 25 Typical Impact Pressure Trace during Run

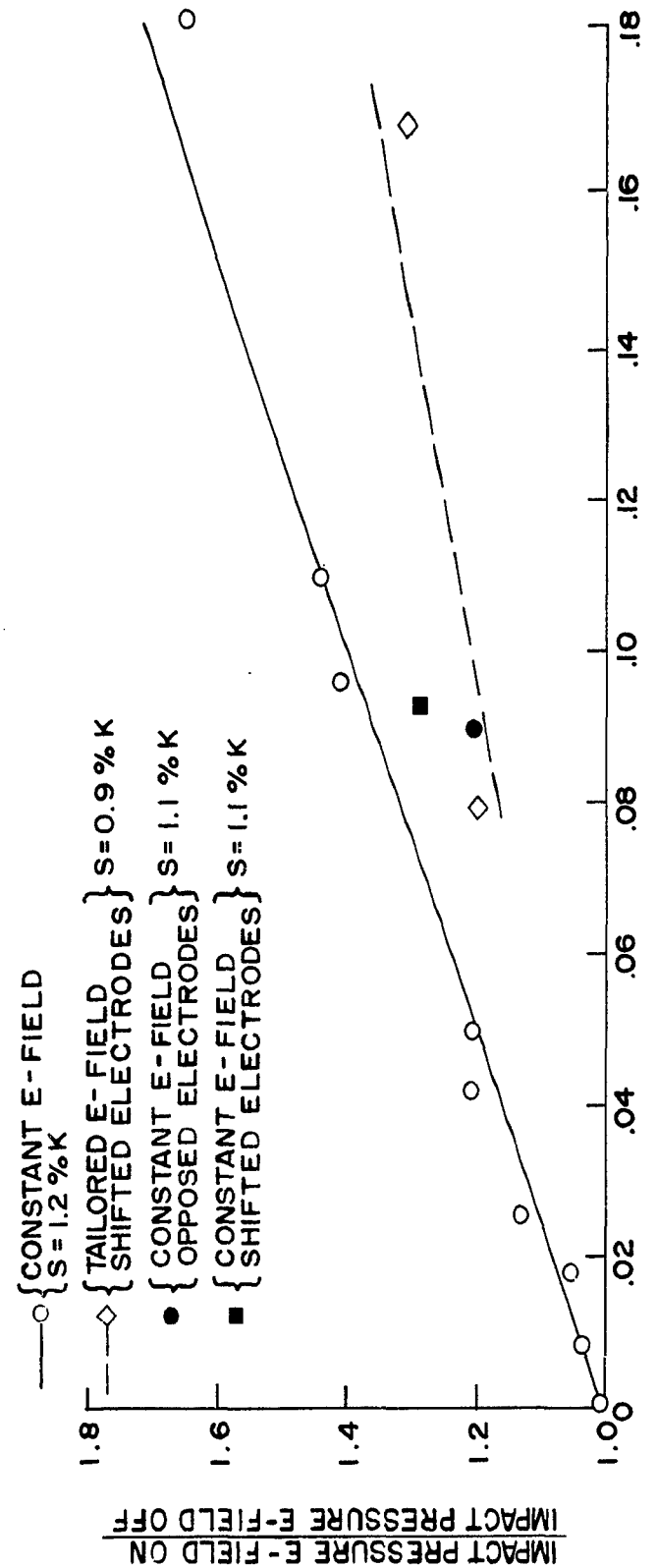

Fig. 26 Impact Pressure Rise as a Function of Input Power for Various Channel Configurations and Operating Conditions

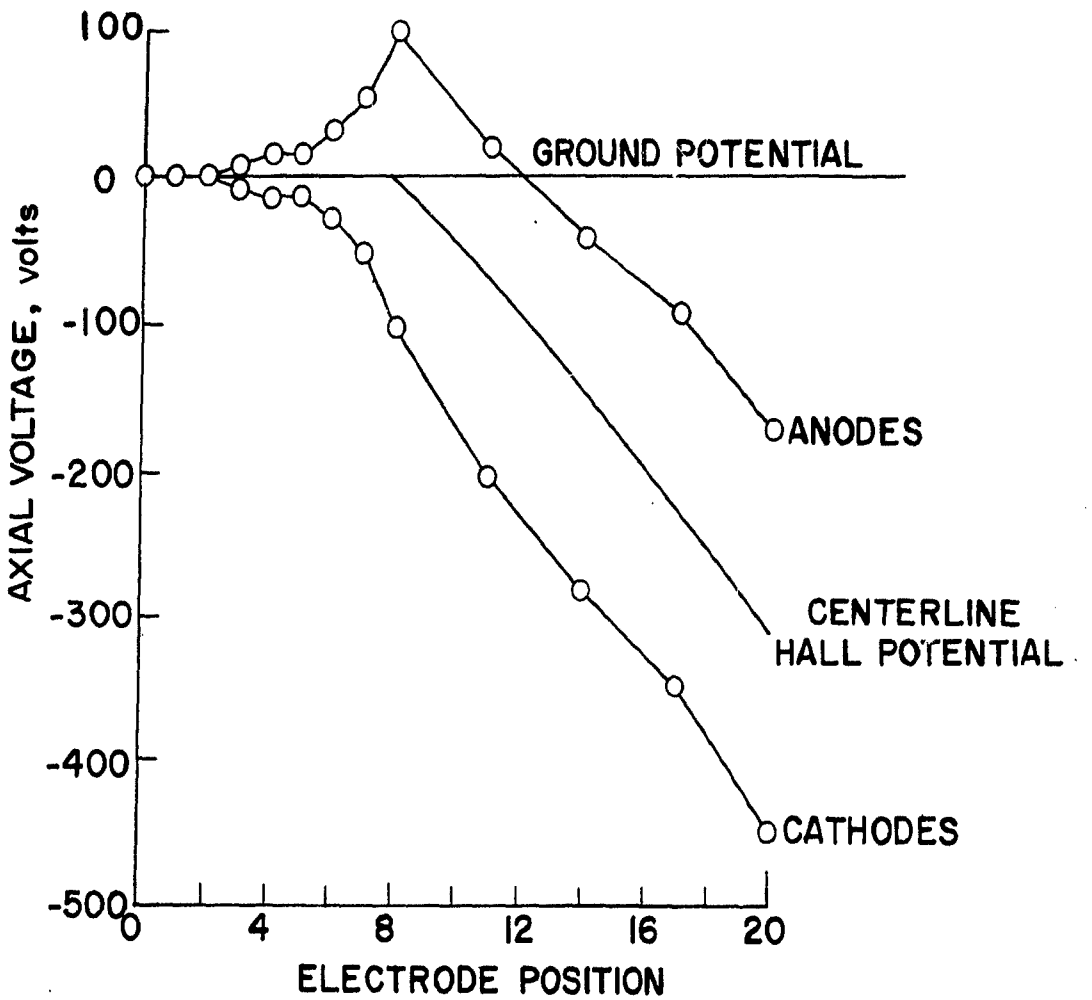

Fig. 27 Typical Axial Voltage Distribution in 20-Electrode Channel